

UNIVERSITY OF TWENTE.

Development of a phantom set-up for perfusion quantification in X-ray imaging modalities

Studying perfusion imaging in critical limb ischaemia and ischaemic stroke

Supervisors

Prof. dr. S. Manohar
M.E. Kamphuis Msc

Multi-Modality Medical
Imaging group
Faculty of Science &
Technology
University of Twente
P.O. Box 217
7500 AE Enschede
The Netherlands

Liselot Goris
MSc Thesis BME
June 2022



Preface and acknowledgement

Before you lies my master thesis ‘Development of a phantom set-up for perfusion quantification in X-ray imaging modalities.’ This thesis is performed at the Multi-Modality Medical Imaging (M3I) group at the University of Twente (UT), as the final assignment to complete the master’s Biomedical Engineering and specifically the track Imaging and In Vitro Diagnostics. The graduation committee includes prof. dr. Srirang Manohar (chair), Marije Kamphuis (daily supervisor), and prof. dr. -ing Jutta Arens and prof. dr. Riemer Slart (external members).

What I loved about this research project is that it was a real team effort, it would not have been possible without the help and support of numerous people. My biggest appreciation goes to my daily supervisor, Marije Kamphuis, for her guidance and support. Her ongoing enthusiasm for the research field inspired me and made me feel really excited to work on the project. Secondly, I would like to thank my supervisor Srirang Manohar for his valuable input and suggestions throughout this project.

I am also very grateful for the technical support during the design and realisation of the phantom set-up from Henny Kuipers and Johan van Hespen. Furthermore, I want to thank Jaap Greve and Remko Liefers for their support and input during the testing phase at the University of Twente. Special thanks go to Bryan Wermelink who showed me the clinical value of the work and was always willing to help me out with questions.

This research was in collaboration with the Universitair Medisch Centrum Groningen (UMCG) who, together with Marije Kamphuis, initiated the project. From this group, I would, first of all, like to thank Abdallah Zaid Al-Kaylani, with whom I worked in close collaboration and who helped me out with the CT perfusion measurements. I would like to extend my thanks to Reinoud Bokkers, Richte Schuurmann, and Marcel Greuter for their useful input during our monthly meetings and the times we met in Groningen. Furthermore, I would like to acknowledge the support of Jan Braaksma, who took the time to help us with the CT perfusion measurements at the UMCG.

Last of all, many thanks to my friends and family. To my (bonus-)parents for always listening to my stories, and letting me drive in their car to Groningen. To my friends of the triathlon associations who helped me clear my head. To Jasmin Siersema for her input on the design of the report. And, to all the students in the ‘afstudeerders hok,’ you provided a great atmosphere to work in.

Abstract

Purpose The ultimate goal of this research is to facilitate ground-truth evaluation of image-derived tissue perfusion measures in the clinical setting. This work focuses on the development of a perfusion phantom set-up dedicated to angiographic imaging of the microcirculation in the lower extremities and computed tomography (CT) perfusion imaging of the brain.

Methods This study contains the design, realisation and testing of the phantom set-up. The phantom is designed for 3-D printing and comprises a vessel structure which branches into two microcirculation compartments that can be filled with a material of choice. The interchangeable phantom is build into a flow circuit in which the flow can be controlled and measured with flow sensors, a perfusion defect can be simulated by adjusting the resistance. The reproducibility, effect of a perfusion defect, effect of flow velocity, effect of imaging protocol and effect of imaging system was tested on two different C-arm CT imaging systems. Proof of concept tests were performed with multidetector CT for perfusion imaging and the associated clinical software.

Results With the phantom set-up realistically shaped and reproducible time-intensity curves (TICs) were acquired in 2-D perfusion imaging, small standard deviations in time-intensity variables between repeated experiments (<4.4%) were observed. Imaging system specific features were found to be negatively affecting the intensity variables, reducing the reliability of the imaging technique for perfusion quantification based on intensity values. In the CT perfusion measurements TICs were obtained with the clinical software, the calculated flow and volume were directly related and a promising correlation between the computed and measured flow was found ($\rho = -0.98$, $p=0.01$). However, the shape and values of the TICs do not resemble the values of human cerebral perfusion data yet.

Conclusions A versatile perfusion phantom set-up applicable for 2-D perfusion angiography imaging is designed and realised. With small changes the set-up could be suitable for multi-modality and multi-disease purposes and may provide necessary insights in perfusion imaging techniques.

Samenvatting

Doel Het ultieme doel van dit onderzoek is het realiseren van een kwantitatieve perfusie maat vanuit beeld afgeleide perfusie metingen in een klinische setting. Dit werk richt zich op de ontwikkeling van een perfusie-fantoom-opstelling gericht op angiografische beeldvorming van de microcirculatie in de onderste ledematen en computertomografie (CT) perfusie beeldvorming van de hersenen.

Methode Deze studie omvat het ontwerp, de realisatie en het testen van de fantoom-opstelling. Het fantoom is ontworpen voor 3-D printen en bestaat uit een vaatstructuur die vertakt in twee microcirculatiecompartimenten, die gevuld kunnen worden met een materiaal naar keuze. Het verwisselbare fantoom is ingebouwd in een stromingscircuit waarin de flow kan worden gecontroleerd en gemeten met flowsensoren. Een perfusiedefect kan worden gesimuleerd door de weerstand aan te passen. De reproduceerbaarheid, het effect van een perfusiedefect, effect van de stroomsnelheid, effect van het beeldvormingsprotocol en effect van het systeem is getest op twee verschillende C-arm CT- systemen. Proof of concept-tests voor perfusie beeldvorming op multidetector-CT en de bijbehorende klinische software zijn uitgevoerd.

Resultaten De fantoomopstelling realiseert reproduceerbare en realistische tijds-intensiteitscurven (TICs) met 2D-perfusiebeeldvorming. Kleine standaarddeviaties in tijdsintensiteitsvariabelen tussen herhaalde experimenten (<4,4%) werden waargenomen. Specifieke kenmerken van het beeldvormingssysteem bleken een negatieve invloed te hebben op de intensiteitsvariabelen, hierdoor lijkt de betrouwbaarheid van perfusie kwantificering op basis van intensiteitsvariabelen laag te zijn. In de CT-perfusiemetingen werden TICs verkregen met de klinische software, de berekende stroom en volume waren direct gerelateerd en een veelbelovende correlatie tussen de berekende en gemeten stroom werd gevonden ($\rho = -0,98$, $p=0,01$). Echter, de vorm en waarden van de TICs vertonen nog niet genoeg overeenkomst met de menselijke cerebrale perfusie curves.

Conclusies In dit onderzoek is een veelzijdige perfusie fantoomopstelling, toepasbaar voor 2-D perfusie angiografie, ontworpen en gerealiseerd. Met kleine aanpassingen zou de opstelling geschikt kunnen zijn voor meerdere modaliteiten en ziektebeelden, en kan deze de nodige inzichten verschaffen in perfusie beeldvorming.

Abbreviations

2-D	2-dimensional	MRI	Magnetic resonance imaging
3-D	3-dimensional	MRI PWI	Perfusion- weighted magnetic resonance imaging
ABI	Ankle-brachial index	MTT	Mean transit time
ABS	Acrylonitrile butadiene styrene	PAOD	Periferal arterial disease
AIF	Arterial input function	PD	Peak density
AUC	Area under the curve	PI	Perfusion imaging
BF	Blood flow	PLA	Polyactic acid
CBCT	Cone beam CT	POM	Polyoxymethylene
CBF	Cerebral blood flow	ROI	Region of interest
CBV	Cerebral blood volume	SLA	Steriolithography
CLI	Critical limb ischeamia	SLS	Selective laser sintering
CT	Computed tomography	SVD	Singular value decomposition
CTP	Perfusion CT	TIC	Time intensity curve
DSA	Digital substraction angiography	TOA	Time of arrival
FDM	Fused deposition modeling	TTM	Time to max
HU	Hounsfield unit	TTP	Time to peak

Table of contents

Preface and acknowledgement	i
Abstract	ii
Abbreviations	iv
1 Introduction	1
2 Background	3
2.1 Critical limb ischaemia	3
2.2 Brain Ischaemia	5
2.3 Perfusion imaging in (tomographic) X-ray systems	6
2.4 Perfusion phantoms	12
3 Developing a phantom set-up: Design Method, Market Research and Requirements	13
3.1 Method: the design circle	13
3.2 Market Research	15
3.3 Phantom requirements	19
4 Phantom design and realisation	22
4.1 Phantom design	22
4.2 Initial testing of the phantom set-up	31
5 Testing the phantom: studying 2- dimensional phantom perfusion imaging with C-arm angiography	36
5.1 Analyses method: semi-automated two-dimensional perfusion analyses in MATLAB	36
5.2 Proof of concept and comparison with clinical values	39
5.3 Reproducibility of the phantom set-up	41
5.4 Effect of perfusion defect	45
5.5 Effect of flow velocity	45
5.6 Effect of imaging system	46
5.7 Effect of imaging protocol (framerate)	48
5.8 Scaling of the system	49
5.9 Conclusions of 2-D phantom perfusion measurements	51

6	Testing the phantom: studying 3 - dimensional phantom perfusion imaging with CT	53
6.1	Analyses method: application of clinical software in CT perfusion measurement	53
6.2	First measurements and corrections to be made	53
6.3	Re-design: phantom enhancements for recognition by the clinical software	54
6.4	Second set of experiments and conclusions	55
7	Discussion and conclusion	62
7.1	Phantom design and realisation	62
7.2	Phantom testing and evaluation	63
7.3	Validation and application	64
7.4	Conclusion	64
	References	65
	Appendix A Appendix A: Phantom requirements	70
	Appendix B Appendix B: Comparison Chart	72
	Appendix C Appendix C: Analyses method in Matlab	74
	Appendix D Appendix D: Workflow Syngo.via	77

1 | Introduction

The human body's circulatory system contains almost 100.000 kilometers of blood vessels. [1] Every minute five litres of blood are pumped out of the heart into this circulatory system of arteries, arterioles, capillaries, venules and veins. [2] The perfusion of organs and tissue happens at the microcirculatory level, oxygen and nutrients will pass through the thin walls of the capillaries, and carbon dioxide and waste products will be removed from the tissue. Therefore, a correct operation of the microcirculatory system is vital for the organ functioning.

In the Netherlands, 25% of all deaths can be attributed to cardiovascular disease. [3] A major cause of cardiovascular disease is (the effect of) atherosclerosis: a thickening or narrowing of the arteries caused by the buildup of plaque in the vessel wall. [4] Once the vessel wall gets thicker, the blood flow will be reduced, eventually ischaemia can occur in the affected region. In general, cardiovascular disease management is essential to prevent deterioration of the disease and eventual ischaemic outcomes. Disease management is a continuous process and includes diagnosis, monitoring of the disease, and interventions. Correct diagnosis is essential for risk assessment and drawing up the treatment plan. Monitoring the course of the disease is important to adjust the treatment plan on time and decide on when to plan interventions. During interventions monitoring also plays an important role to guide the clinician in decision making. Developments in all of these parts of disease management can play a role in improving clinical outcomes.

In this research we focus on two clinical cases of cardiovascular disease where disease management might be improved: stroke and critical limb ischaemia. In the case of a stroke every second counts, a decrease in brain perfusion may cause irreversible brain damage within minutes. [5] Reducing the time between diagnostics and intervention could save millions of neurons. [6] At the moment, perfusion computed tomography (CT) or perfusion-weighted magnetic resonance imaging (MRI PWI) are recommended by international guidelines [7] to define the affected brain tissue before intervention is initiated. A possibility to save time could be by imaging and evaluating brain perfusion at the interventional suite and discharge the extra stop for diagnosis with perfusion CT or MRI PWI. In this way revascularisation can also be evaluated during intervention, preventing re-intervention. Cone-beam CT (CBCT) C-arm systems could be used for this purpose, an earlier study showed that when the temporal sampling/resolution is improved and noise is reduced during post-processing, perfusion data of a biplane flat detector angiographic system was suitable to establish clinically usable perfusion maps. [8] To research if it would be possible to use CBCT for diagnosis and evaluation of ischemic stroke (treatment), a comparison needs to be made between the current imaging modality, perfusion CT, and the perfusion maps obtained with CBCT.

In 50-60% of patients with critical limb ischaemia (CLI) a revascularisation procedure needs to be performed to restore the blood flow to the affected limbs. However, intervention does not always fully recover perfusion, and amputation rates are high: 15-20% at 1 year. [9] Amputation is a costly procedure, both concerning the impact on the patient's life as well as financial costs. At present, it is hard to foresee if revascularisation intervention is successful. In the ideal situation, a quantitative perfusion measure can indicate if revascularisation was successful during surgery. The revascularisation is performed in the angiography suite and is primarily aimed at revascularisation and imaging of the blood flow (BF) in the macrocirculation. However, CLI is caused by restricted blood flow to the affected tissue due to impaired regulation of both macrovascular and microvascular regulation. [10] When re-perfusion of the macrovascular regulation is achieved, microvascular regulation could still be damaged and CLI will not recover. Including measurements of (re)-perfusion in microvascular regulation into the imaging protocol of endovascular procedures could possibly be used to help the surgeon in decision making. [10, 11] Ultimately, this might reduce rehospitalization and amputation rates. Nevertheless, a quantitative measure and imaging protocol for the quantification of revascularisation in microcirculation is still lacking. [10]

To research such a quantitative measure phantom studies could be carried out. A phantom study could provide a controlled, simplified and reproducible environment to simulate the macro- and microcirculation. In this way, ground truth perfusion values can be evaluated. Compared to human or animal studies a phantom can provide consistent results and is more easily available, the phantom study can provide insights in- and be used for the validation of imaging techniques. A phantom could also be used to simulate pathologies, such as a perfusion defect, and gain insights in the differences with a healthy situation. Furthermore, a medical imaging phantom could be used to study cerebral perfusion imaging in CT and CBCT and compare the modalities.

The aim of this study was to develop a perfusion phantom set-up that could be used to study perfusion imaging of the microcirculation of the lower extremities with angiography and cerebral perfusion with CT perfusion. The main focus was to develop a perfusion set-up of the vascularisation of the lower extremities and studying quantitative perfusion imaging with C-arm angiography in a controlled environment. The secondary goal was to study quantitative perfusion imaging of the vascularisation of the brain with CT perfusion by making small adjustments to the phantom set-up. When successful, this set-up can in the future be used for defining a validated CT perfusion standard and comparing the measurements (as golden standard) to study quantitative perfusion imaging with cone beam CT. The objectives of this study include:

1. Determining the program of requirements for the generic phantom set-up
2. Translating the program of requirements to a design of the phantom set-up
3. Testing and evaluating the phantom set-up on the program of requirements for the aforementioned clinical cases

This study was performed by following the iterative process of a design circle, i.e., after the identification of the problem we researched the problem, drew up the program of requirements, generated possible solutions, selected the best solution and build and tested the set-up, new problems were identified and a new iteration was followed. The end product was evaluated and future recommendations were made.

2 | Background

This chapter contains the clinical and in-depth technical background of this research. The clinical context of critical limb ischaemia and brain ischaemia will be outlined and the technical background of perfusion imaging in (tomographic) x-ray systems is described.

2.1 Critical limb ischaemia

Peripheral arterial occlusive disease (PAOD) is a medical condition in which the arterial perfusion of the distal portion of the aorta, pelvic, femoral, or crural arteries is decreased, due to a blockage or narrowing, mostly caused by atherosclerosis. [12] Worldwide over 200 million people are diagnosed with PAOD. [13] Up to 25% of patients suffering from PAOD experience symptoms like fatigue and claudicatio intermittens (CI) (pain and cramping sensations when exercising) [13]. Critical limb ischaemia (CLI) is one of the last stages of PAOD. In CLI, capillary bed perfusion cannot be sufficiently maintained due to damage to the macro- and microcirculation, resulting in tissue ischaemia, which induces pain at rest and poor wound healing. [14] In figure 2.1 the formation of the atherosclerotic plaque and effect is schematically shown. The different stages of PAOD are defined in the Fontaine stages and Rutherford categories (table 2.1). CLI is classified by Fontaine stage II or IV. [12]

Diagnosis of PAOD and CLI relies on history, physical examination, and the ankle-brachial index (ABI). Cardiovascular disease, diabetes mellitus, age, family history, and smoking increase the risk of PAOD. [15] During the physical examination, the blood flow in the lower limb is assessed, and the temperature, muscle strength, volume, and shape of the lower extremities are examined. The ABI is used as a diagnostic measure for PAOD and is determined by dividing the highest systolic blood pressure in the ankle (of the affected side) by the highest systolic blood pressure in the arms. The patient is diagnosed with PAOD if $ABI < 0.9$. Diagnosis of CLI is established when the patient experiences pain at rest, and/or has skin abnormalities at the lower limb and the systolic Doppler ankle pressure is smaller than 50 mmHg. [16]

Table 2.1 Fontaine and Rutherford classification of PAOD [12]

Fontaine		Rutherford		
Stage	Clinical manifestations	grade	category	Clinical manifestations
I	asymptomatic	0	0	asymptomatic
II a	can walk >200m	I	1	mild claudication
II b	can walk <200m	I	2	moderate claudication
		I	3	severe claudication
III	ischemic pain at rest	II	4	ischemic pain at rest
IV	ulcer, gangrene	III	5	small area of necrosis
		III	6	large area of necrosis

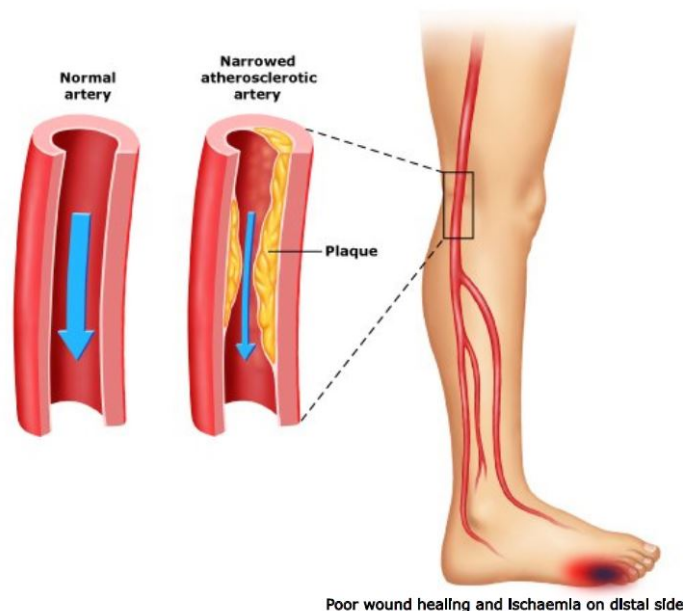


Fig. 2.1 Critical limb ischaemia: the formation of an atherosclerotic plaque which restricts the blood flow towards the lower leg and foot, causing poor wound healing and ischaemia of the tissue. Image adjusted from [17].

Treatment of the early stages of PAOD focuses on vascular exercise and controlling cardiovascular risk factors. [12] In the case of intermittent claudication, invasive treatment can be decided upon. In case of CLI, 50-60% of patients are hospitalized within 6 months to undergo revascularisation intervention (surgical or endovascular). However, intervention does not always fully recover perfusion, and amputation rates are high: 15-20% at 1 year [9]. Amputation is a costly procedure, both concerning the impact on the patient's life as well as financial costs. At present, it is hard to foresee if revascularisation intervention is successful. In the ideal situation, a quantitative perfusion measure can indicate if revascularisation was successful during surgery, and guide the surgeon in decision making.

2.2 Brain Ischaemia

Every year 40,000 people in the Netherlands are affected by stroke [18]. It is the fourth most common cause of death and one of the most important causes of persisting invalidity. In 20% of the cases, stroke is caused by intracerebral bleeding (hemorrhagic stroke). In the other 80% of the cases, stroke is caused by an occlusion of blood vessels feeding into the brain (ischemic stroke). [19] The blockage of the arteries is caused by a blood clot, which is often formed in arteries that are damaged by atherosclerosis (figure 2.2). In both hemorrhagic- as well as ischemic strokes the disturbed blood supply rapidly causes brain damage (within minutes) and can lead to disability or death. It is therefore extremely important to diagnose stroke on time and initiate treatment.

The diagnosis of stroke is done using magnetic resonance imaging (MRI) or computed tomography (CT) to find the cause of stroke and draw up a treatment plan. In ischemic stroke perfusion-weighted MRI or CT can identify the affected tissue; a differentiation is made between the ischemic core and the surrounding penumbra: moderately ischemic tissue with damaged electrical activity but maintained cellular metabolism, which can be recovered when reperfusion is achieved within 6-8 hours. [20]

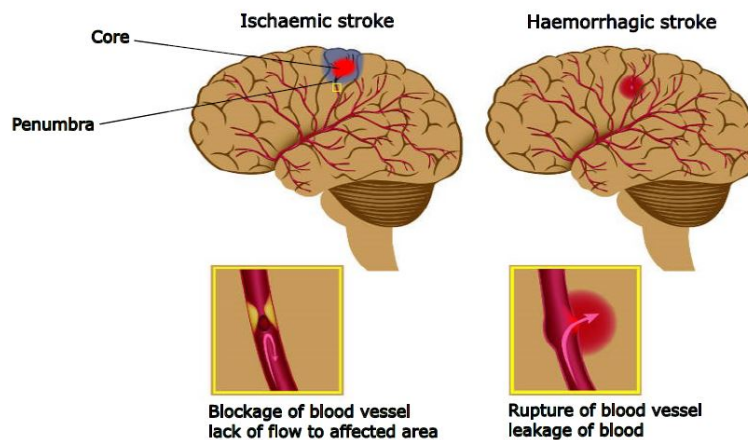


Fig. 2.2 The causes of ischaemic stroke vs hemorrhagic stroke. In ischaemic stroke a differentiation is made between the (irreversible) ischaemic core (red area) and the surrounding penumbra (blue area, which can recover when reperfusion is achieved within 6-8 hours). Image adjusted from [21].

Treatment of ischemic stroke is aimed at removing the blood clot and restoring perfusion. This can either be done with intravenous medication that breaks up the blood clot or endovascular procedures. The endovascular procedures are performed in the angiographic suite. Medication can be directly delivered to the brain with a catheter or the clot can be removed with a stent retriever attached to a catheter. In both cases, C-arm CT is used for image-guided therapy.

2.3 Perfusion imaging in (tomographic) X-ray systems

Perfusion imaging (PI) is an important functional-imaging method to assess the vascular status of the tissue. PI can be applied to multiple imaging modalities, such as MRI and CT, to assess perfusion by the representation of a time-intensity curve (TIC) of the contrast volume flow in tissue (figure 2.3). A TIC is the representation of the average relative intensity of a voxel in the ROI over time. From the TIC perfusion parameters can be extracted, which can be used to assess the perfusion status of the tissue. The most commonly used parameters include:

- Area under the curve (AUC): a measure for the amount of volume flowing through the region of interest (ROI). The AUC increases after revascularisation [11, 22]
- Maximum slope of the curve: maximum slope between time of onset of the contrast inflow and the time of peak enhancement [23]
- Mean transit time (MTT): time from the wash-in to the wash-out of the contrast agent. MTT is prolonged in an ischaemic area [23]
- Peak density (PD): the maximal blood volume (BV) and density in the ROI. The PD increases after revascularisation [11, 22]
- Time of arrival (TOA): time between the first frame of the TDC and the time at which the contrast is detected [23]
- Time to peak (TTP): time to the apex of the curve (at maximum intensity). The TTP is decreased in case of obstruction or stenosis [23]

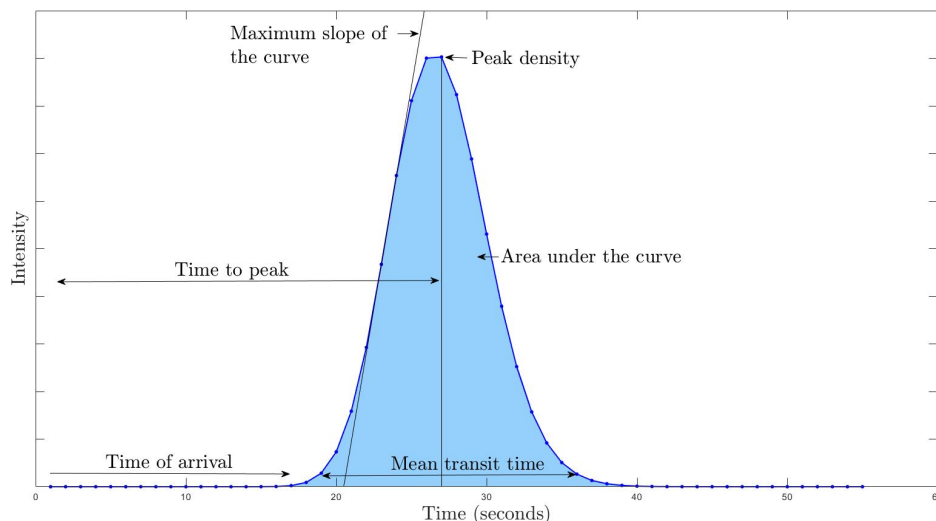


Fig. 2.3 Time-intensity curve showing the most commonly used perfusion parameters

Time to peak is the time to the maximum intensity of the curve, peak density is the maximum intensity, time of arrival is the time until the wash of contrast in the region of interest (ROI) and mean transit time is the time between the wash in and wash out of the contrast in the ROI

In this research, we focus on perfusion imaging in (tomographic) X-ray systems, more specifically CT perfusion and C-arm CT systems. CT perfusion is used for the assessment of brain perfusion and measures the CT attenuation in the brain after applying a contrast dosage. C-arm CT systems are used in the angiography suite, with these systems two-dimensional images can be made using techniques such as fluoroscopy and digital subtraction angiography (DSA). In the newer C-arm CT systems three-dimensional Cone Beam CT images can be acquired. This chapter contains an elaboration on the different imaging techniques and their role in PI.

2.3.1 Perfusion angiography

Revascularisation procedures are carried out at the angiography suite. During the procedure, a C-arm provides visual details of vascularization and can help to guide the surgeon through complex cases. A contrast agent is injected into the bloodstream, the contrast agent will move to the region of interest. The first fluoroscopy image is used to make a mask which is subtracted from the series of consecutive fluoroscopy images: this is called digital subtraction angiography (DSA). When making fluoroscopy images the degree of perfusion of the macrocirculation can be (qualitatively) assessed. This assessment depends on the interpretation of the vascular surgeon and is subjective: there is a clinical need for quantitative measures for both macrovascular blood flow and microvascular perfusion during surgery. Such a measure could help the surgeon in decision-making during surgery and improve clinical outcomes. Perfusion angiography could possibly provide the tools for this measure: TICs could be computed of the region of interest on the 2-D angiography images and the TIC values could be related to clinical outcome [23, 22]. A perfusion phantom could provide a standard environment to validate TIC values of 2-D angiography measurements.

2.3.2 CT perfusion

In computed tomography, a rotating X-ray tube sends out X-rays over different angles. The X-ray attenuation of the tissue under investigation is measured over these angles with a row of detectors placed in a gantry. The acquired attenuation profile over different angles (sinogram) is processed using reconstruction algorithms, resulting in tomographic images (slices) of the tissue. These tomographic images can be combined to obtain 3-D volumes. In the case of CT perfusion (CTP) a contrast agent is administered intravascularly and is tracked during its first circulation through the tissue capillary bed of the organ of interest.[24] After injection the contrast agent travels through the arteries into the tissue and out via de veins again. From the arterial input and venous outflow of contrast functions can be drawn up: the arterial input- and venous outflow function. The main interest is however the tissue concentration of contrast, to describe tissue capillary level blood flow. In the next sections the computation of tissue perfusion parameters is explained.

Calculations on CT perfusion: computation of tissue perfusion parameters

With CT perfusion certain perfusion parameters to describe tissue capillary level blood flow can be determined, these include the ones described in section 2.3 and (in the case of the brain) cerebral blood volume (CBV) and cerebral blood flow (CBF). CBV is the amount of milliliters of blood per 100 gr of tissue. CBF is the amount of milliliters of blood per 100g of brain tissue per minute. The MTT is defined by the CBV divided by the CBF, it is de average passage time (sec) of the blood between the arterial inflow and venous outflow. In CT perfusion calculation models, it is assumed that the perfusion tracer is not diffusible, not metabolised and not absorbed by the tissue it traverses through. [24] This holds in the healthy situation, however, in the case of malignancies certain amounts of tracer can ‘get lost.’ For example: in case of infection or inflammation the

blood-brain barrier can get broken down and the tracer can leak into the extravascular space, which results in an overestimation of the cerebral blood volume (CBV) [25]. An elaboration on the calculation methods of CBV and CBF is included in the next sections.

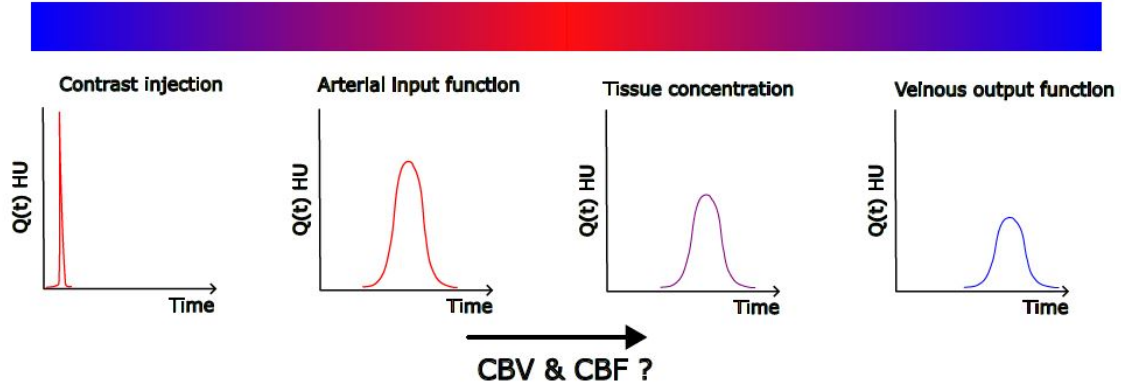


Fig. 2.4 In CT perfusion imaging a contrast agent is injected in the veins, after which it travels through the heart towards the arteries. From the artery of interest an arterial input function is computed, with the contrast concentration ($Q(t)$ in HU) on the y-axis and the time on the x-axis. The contrast agent travels from the artery towards the tissue. A venous output function can be computed from venous outflow. The cerebral blood volume (CBV) and cerebral blood flow (CBF) can be computed using different approaches.

Determination of CBV

In CTP cerebral perfusion is determined by looking at the relationship between the contrast enhancement of the arterial input, tissue, and venous outflow. From the input and output of the tracer in/of a voxel, the volume distribution (fractional vascular volume, f) can be determined. [24] The fractional vascular volume is defined by the volume taken up by the vascular space divided by the total volume (vascular space, interstitium, and cells altogether) [24]:

$$f = \frac{V_{\text{vasc}}}{V_{\text{vasc}} + V_{\text{interstitium}} + V_{\text{cells}}} = \frac{V_{\text{vasc}}}{V} \quad (1)$$

The tissue contrast concentration (Q_{tissue}), measured with CT, is determined by the intravascular concentration times the fractional vascular volume and is smaller than the vascular concentration [24]:

$$Q_{\text{tissue}} = f \cdot Q_{\text{vasc}} \quad (2)$$

The total volume of contrast material reaching the tissue via the arteries is equal to the CBF times the integral of the arterial concentration, Q_{artery} . Based on the conservation of mass, this is equal to the amount of contrast departing the tissue, the CBF times the integral of the vascular concentration Q_{vasc} [24]:

$$CBF \cdot \int_0^T Q_{\text{artery}}(t) dt = CBF \cdot \int_0^T Q_{\text{vasc}}(t) dt \quad (3)$$

Equation 2 and 3 can be combined:

$$f = \frac{\int_0^T Q_{\text{tissue}}(t) dt}{\int_0^T Q_{\text{artery}}(t) dt} \quad (4)$$

From this equation, the CBV can be calculated. In order to do so, the brain tissue attenuation, ρ , and a correction factor, CH, need to be taken into account. The correction factor is necessary to accommodate for the difference between capillary and arterial hematocrit [24, 26].

$$CBV = \frac{CH}{\rho} \cdot \frac{\int_0^T Q_{\text{tissue}}(t) dt}{\int_0^T Q_{\text{artery}}(t) dt} \quad (5)$$

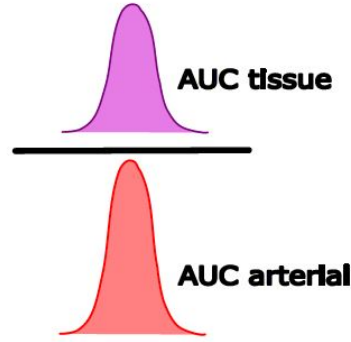


Fig. 2.5 Cerebral blood volume (CBV) can be calculated using the areas under the tissue and arterial time intensity curves

When a steady state between arterial and tissue contrast is established during CT perfusion image acquisition, a change in attenuation due to contrast distribution is proportional to its concentration. When this is the case, the fraction of change in HU value of the brain tissue and in the arterial input can be used to estimate the CBV in milliliters per 100 grams of tissue [24]:

$$CBV = \frac{\Delta HU_{tissue}}{\Delta HU_{artery}} \cdot V_{voxel} \cdot N \quad (6)$$

With N the number of voxels in 100g tissue and V_{voxel} the voxel volume (in cm^3), this is schematically shown in figure cbv. It should, however, be taken into account that nowadays CT perfusion protocols are fast and the injection rate of contrast has become higher, meaning that a steady-state assumption cannot always be made and the perfusion maps should in these cases become more flow weighted than volume-weighted. [24]

Determination of CBF

CBF can be calculated using different approaches, including deconvolution- and nondeconvolution- based methods. Deconvolution-based methods are computationally more challenging, nondeconvolution-based methods are based on simplifications of the vascular architecture, making them less reliable.

Both methods are based on the Ficks principle of the conservation of mass. $Q(T)$ is calculated, this is the accumulated mass of contrast in a voxel between wash in and wash out of a contrast bolus injection. [24]

In the nondeconvolution based method, $Q(T)$ can be calculated by multiplying the CBF with the time integral of the difference between the arterial and venous contrast concentration [24]:

$$Q(T) = CBF \cdot \int_0^T [Q_{artery}(t) - Q_{vein}(t)] dt \quad (7)$$

In this case, it is assumed that there is a single in and outflow, the bolus injection is instantaneous (without delays) and there is no dispersion (there is one path). When the assumption is also made that the venous concentration is zero during the period of time because the contrast did not reach the venous side yet, the equation can be further simplified (known as the Mullani-Gould or single-compartment formulation [27]) [24]:

$$Q(T) = CBF \cdot \int_0^T Q_{artery}(t) dt \quad (8)$$

This equation can be written into the derivative form [24]:

$$\left[\frac{dQ(t)}{dt} \right]_{t=T} = CBF \cdot Q_{artery}(T) \quad (9)$$

Now, the equation (9) can be rewritten, based on the assumption that the contrast accumulation rate is maximal when the arterial concentration peaks. This is called the *maximum-slope method*. [24]:

$$\left[\frac{dQ(t)}{dt}\right]_{Max} = CBF \cdot [Q_{artery}(t)]_{Max} \quad (10)$$

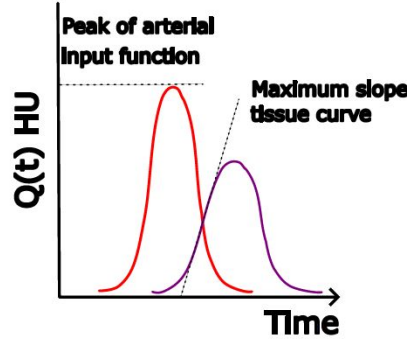


Fig. 2.6 The maximum slope method to calculate the Cerebral Blood Flow (CBF). CBF is equal to the maximum slope of the tissue intensity curve divided by the peak of the arterial input function.

This method (also shown in figure 2.6) for calculating CBF is simple and fast, however, the assumption of no venous outflow does in many cases not hold as very high flow rates of contrast agent injection (> 10 mL/s) are necessary to prevent overlap of the arterial input and venous outflow curve. [24] In practice, flow rates of 5 mL/s are used. As a result, the maximum slope method leads to relative instead of absolute perfusion measures, which makes the comparison of results between patients and institutions difficult. [28]

CBF: Deconvolution based models

In these models the concentration of tracer in tissue $Q_{tissue}(t)$ is described based on two functions [24]:

1. A residue function $R(t)$. A unitless number, describing the fraction of contrast that remains present after the bolus injection in the voxel of interest at time t . Starts at 1 at $t=0$.
2. The arterial input function (AIF) $Q_{artery}(t)$. The concentration of contrast at time t in the incoming vessel for the perfusion of the voxel of interest. Here, the assumption is made that the artery taken for the AIF is responsible for the exact input to the tissue of interest.

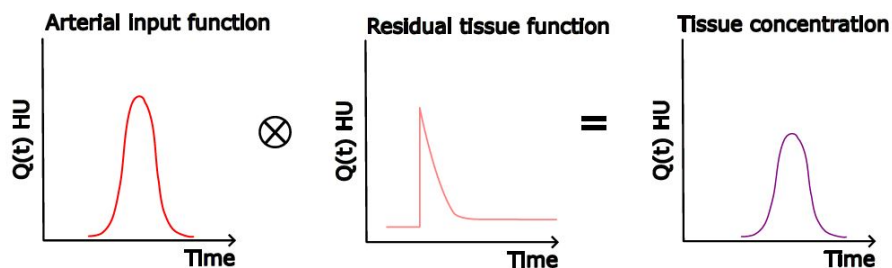


Fig. 2.7 A deconvolution method to calculate the cerebral blood flow (CBF). The arterial input function (AIF) convolved with the tissue residual function, times the CBF and a correction factor is equal to the tissue concentration ($Q_{tissue}(t)$). The AIF and $Q_{tissue}(t)$ can be measured from the time intensity curve.

Meier and Zieler [29] showed that the tissue concentration curve $Q_{tissue}(t)$ can be described by the product of a correction factor, the CBF and the AIF convolved with $R(t)$. Shown in figure 2.7. This equation is based on the statement that the tissue time intensity curve is an expression of the effects of the AIF and inherent tissue properties. Hence, to derive $R(t)$ the effect of AIF should be removed, this can be done using deconvolution.

$$Q_{tissue}(t) = \frac{\rho}{CH} \cdot CBF \cdot [AIF(t) * R(t)] = \frac{\rho}{CH} \cdot CBF \cdot \int_{\tau}^t AIF(\tau) R(t - \tau) d\tau \quad (11)$$

In this equation AIF and $Q_{tissue}(t)$ can be measured directly from the time intensity curve. Solving CBF and $R(t)$ is more complicated. There are several possibilities, including the Fourier Theorem (FT) or Singular Value Decomposition (SVD).[24]

- Fourier theorem: the convolution of two time domain function is equal to multiplying their fourier transforms [24]:

$$R(t) = \frac{1}{CBF} \mathfrak{S}^{-1} \left\{ \frac{\mathfrak{S}[Q_{tissue}(t)]}{\mathfrak{S}[AIF(t)]} \right\} \quad (12)$$

In this case, $R(t)$ is equal to the inverse fourier transform of the ratios of the fourier transformations of the AIF and $Q_{tissue}(t)$. According to Ostergaard et al, this method is very sensitive to noise. [30]

- Singular value decomposition: a method in which the $Q_{tissue}(t)$ equation is rewritten in a matrix form. The matrix vector can be solved using the least-squares method. This method leads to the most robust results for the calculation of CBF. Standard SVD (sSVD) can be adjusted in several ways such as delay- and dispersion-corrected singular value deconvolution (dd-SVD), which corrects for the delay in blood flow from the proximal arteries to the brain tissue [31], and block circulant SVD (bSVD) [32].

Software package variability

As touched upon before, different institutions/commercially available software systems use different methods to calculate the perfusion measures [32]. This results in different perfusion maps when applied to the same patient data. Kudo et al [32], compared the perfusion maps of the same scan generated with five different software manufacturers. In figure 2.8 the results are shown, and the colormap is used for all experiments. The first two sets show the perfusion maps when using two different approaches of singular value decomposition (sSVD and bSVD). A-E are computed by different software manufacturers. The results show a difference between software in areas with CBF decrease, areas with CBV decrease are almost the same among software. In our experiments on the CT FORSE, the SVD method is used.

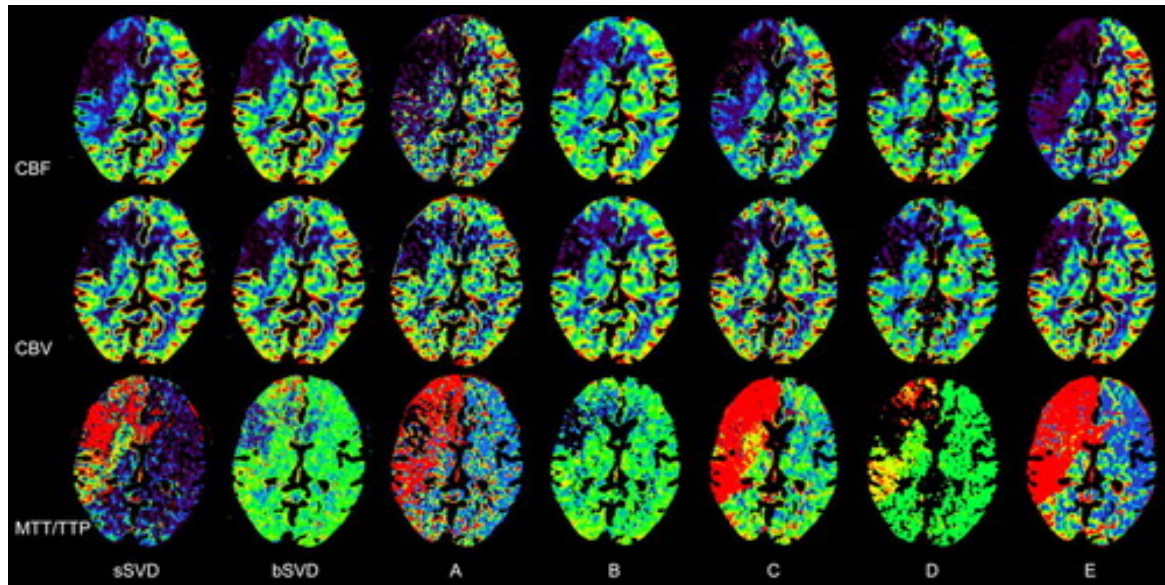


Fig. 2.8 Perfusion maps of CBV and CBF made with different computational techniques and software packages. [32] Showing a difference between software in areas with CBF decrease.

A: GE Healthcare CT Perfusion 3 SVD, B: Hitachi Medical Systems 2.0 IF, C: Philips Medical Systems 1.201 SVD, D: Siemens Medical Systems VA70A MS, E: Toshiba Medical Systems

2.3.3 Cone Beam CT

Nowadays, C-arm CT systems can make cone-beam CT (CBCT) scans. In CBCT scans a cone-beam-shaped radiation field is used and the x-ray modality rotates around the patient. The CBCT 2-D data are collected from projections at different angles and are reconstructed into CT-like images, using filtered back projections. [33] CBCT perfusion imaging has the potential to substitute a CT perfusion stop for patients who come in with a stroke, as in that case all the images can be made at the OR: this reduces waiting times and accelerates treatment in acute settings. However, CBCT has a lower temporal resolution (sampling time of 6 seconds, whereas CT has a sampling time of 1 second) and a limited angle (often 200 degrees instead of 360 degrees). The question remains to what extent the CT perfusion images of CBCT can be compared to those of conventional CT. A perfusion phantom could provide a standardized and reproducible environment to compare the modalities and find out if the temporal resolution is sufficient.

2.4 Perfusion phantoms

Phantoms can be classified into three different configurations based on their complexity: basic phantoms, aligned capillaries, and tissue-filled phantoms. Furthermore, two subclasses can be distinguished: mono- or multi-compartment phantoms. [34] *Basic perfusion phantoms* are relatively simple models consisting of a single volume with in-going and out-going tubes. They mostly neglect the physiological characteristics of microcirculation and tissue. [34] *Capillary phantoms* are used to simulate the microcirculation, using a volume filled with unidirectional hollow fibers or straws, for this purpose dialysis cartridges can be used. [34] The number of fibers, permeability, and diameter varies depending on the simulated tissue. In *tissue-filled phantoms* the volume is filled with material similar to the tissue which needs to be simulated and forms a microvasculature. Materials that can be used are e.g. sponges, microbeads, and gels. [34]

3 | Developing a phantom set-up: Design Method, Market Research and Requirements

3.1 Method: the design circle

The goal of this master assignment was to develop a perfusion phantom setup that could be used to study perfusion imaging of the vascularisation of the lower extremities with C-arm angiography and of the vascularisation of the brain with perfusion CT. In order to reach the goal a development process was composed (figure 3.1).

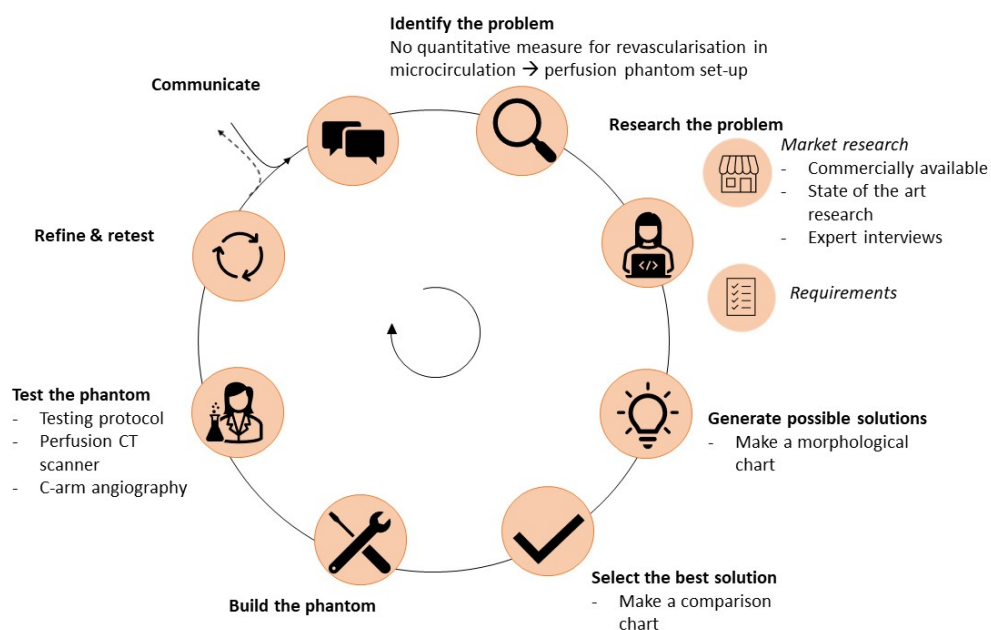


Fig. 3.1 Phantom development process showing the design circle with the steps that are taken to get to a phantom set-up

1. First, the problem was identified and described (chapter 2.1 and 2.2).
2. Thereafter, the problem was researched:

- A market research was done (chapter 3.2): expert input was gathered to find out what the clinical demand of the perfusion phantom setup is and which requirements it needs to fulfil, we looked into the commercially available phantoms, and the state-of-the-art research.
 - With the information gathered during the market research, the next steps could be taken in drawing up the requirements. First, a task analysis was carried out. Answering questions such as: *what do we want to measure? How do we want to measure it? When do we want to measure it?* Thereafter, some tests on a very basic phantom setup were performed with C-arm angiography to get a first impression of practical phantom requirements. The requirements can be found in chapter 3.3.
3. After drawing up the requirements, possible solutions were generated (chapter 4). A morphological chart was made to generate several possible solutions. A comparison chart, with on the left side the requirements and on the other side, the possible solutions were used to choose the best solution.
 4. Once the best solution was chosen the phantom setup was realised.
 5. Perfusion images of the phantom setup were made with C-arm angiography (chapter 5). A testing and analyses protocol was written beforehand (chapter 5.1). When these tests were gone well, perfusion images of the phantom setup were made with perfusion CT (chapter 6). After the first tests, the testing process was refined and new tests were performed.
 6. The final result was communicated to the team and recommendations were made (chapter 7).

After completing the design circle once, the results were evaluated and potential problems were identified. The goal was to complete the circle again with additional phantom requirements to improve the phantom set-up.

3.2 Market Research

Phantom studies could provide a platform for validation of perfusion measures and development/comparison of imaging protocols (across multiple modalities). In this study, we are primarily interested in developing a perfusion/flow phantom set-up of the vascularisation of the lower extremities and studying quantitative perfusion imaging with the C-arm in a controlled environment. Furthermore, we want to be able to adjust the setup to study quantitative perfusion imaging of the vascularisation of the brain with CT perfusion. To develop such a set-up it is important to perform market research. In this way, the viability, feasibility, and desirability of the study can be determined. This market research consists of three parts. Knowledge from expert input, commercially available phantoms, and literature on perfusion phantoms. The market research is limited to perfusion phantoms of the brain and lower extremities.

3.2.1 Expert input

The aim of the expert input was to find out what the clinical demand of the perfusion phantom is and what requirements the phantom needs to fulfill. To gather this information interviews were taken, the questions are listed in figure 3.2. The first category contains questions regarding the clinical demand, disease characteristics, and current workflow. The second category contains technological questions. A vascular surgeon, an interventional radiologist, a clinical physicist and two technical physicians were interviewed.

From the interviews, it was concluded that the extent of revascularisation of the macro-vascularisation is not measured quantitatively but judged visually by the surgeon, based on the blood flow velocity visible on the angiography images. At the moment, it is not possible to acquire a reliable quantitative measure of microcirculation perfusion during revascularisation procedures. A quantitative measure for both the perfusion of the macrocirculation as well as the microcirculation in the lower extremities could possibly help the surgeon in decision making and improve patient outcomes and therefore likely reduce re-interventions. At present, most C-arm CT systems do not have the required temporal resolution to capture a time-intensity curve. However, Siemens claims that their new Siemens Artis Icono C-arm has the required temporal resolution. A phantom study is required to prove this claim. The answers to the technical questions are used to draw up the requirements of the phantom.

Vascular Surgeons/ Interventional Radiologists	Clinical Physicists and Technical Physicians
<ul style="list-style-type: none"> • Why would you like a quantitative measure of micro-circulation perfusion during surgery? What would you like to measure? • Why should the phantom be applicable for both CT perfusion as well as CT-angiography? • Which measures are acquired from the CT-angiography images during surgery? • Is there already a quantitative measure available for the vascularisation in the macrovasculature during revascularisation surgery? • How could the revascularisation procedure be improved? What is missing or can be improved on the technical side? • CT-angiography results in 2D images of the vessels. Does it frequently occur that revascularisation seems to be achieved when looking from a certain angle but is not sufficient when looking from a different angle? • Is insufficient perfusion of microcirculation (after a first attempt of revascularisation) mainly due to a blockage of the macro-circulation or a blockage of the micro-circulation? • Is the anatomy of vessels in the lower extremities patient-specific? Or generalisable? • How does the anatomy of vessels in the lower extremities change in the pathological situation? • Which techniques are used to image perfusion pre-operatively? • How does the blood flow change in case of stenosis? • What contrast flow settings are used? • How does the blood circulation in the brain differ from the blood circulation in the lower extremities? 	<ul style="list-style-type: none"> • Why is it not possible to image micro-circulation perfusion during surgery? • How can one acquire time-density curve information from C-arm data? • What information is included in the C-arm imaging protocol? • What is the difference between the new C-arm (ARTIS icono Siemens) and the old C-arm? • What is measured during a CT perfusion protocol? How large are the ROIs? • What are the typical values for the wash in rate, MTT, and TTP in the microvasculature of the brain and foot? • What software is used to analyse CT perfusion images?

Fig. 3.2 Expert interviews questions

3.2.2 Commercially available phantoms

Commercially there are different CT perfusion phantoms available. These phantoms mainly focus on brain perfusion and are developed to study imaging systems. Sun Nuclear [35], Go To Peo [36] and Simultec [37] developed CT perfusion phantoms which can generate time-intensity curves after a contrast bolus is injected into a region of interest. Figure 3.3 shows the commercially available perfusion phantoms. Sun Nuclear [35] and Go To Peo [36] designed three separate regions of interest, which mimic an artery, a vein, and brain tissue. The regions of interest are not connected. With these commercially available phantoms one can research if the CT scanner provides consistent results and compare CT scanners of different manufacturers. However, they are not designed to be able to get to an absolute measure of perfusion from the measures of the generated time-intensity curves. Simultec [37] manufactured a perfusion phantom based on the research of Driscoll et al [38]. In this research a dynamic flow phantom was designed based on the Tofts kinetic model [39]; This model describes tissue perfusion as a process in two compartments: the intravascular space and the extra vascular space. The phantom consists of two compartments where exchange can take place through small holes, contrast agent arrives via the input tube and leaves via the output tube. This phantom can generate reproducible time-intensity curves. However, there is no homogeneous uptake of contrast agent and it simulates the physiology as if the contrast agent can leave the bloodstream. [38]



Fig. 3.3 Commercially available perfusion phantoms

(a) and (b) contain separate modules to simulate the arteries, veins and microcirculation, in (c) fluid can flow through the 'arterial tube' into the microcirculation compartment and out via the 'venous' tube

3.2.3 State of the art research

In prior work at the university hospital of Groningen a scoring algorithm for in-vitro brain perfusion models was established [40], and a systematic review of brain perfusion/flow phantoms was performed [41]. This research contained a list of different brain perfusion phantoms and an elaboration on the designs and outcomes. Each phantom was scored based on a list of requirements. The systematic review was performed to find out if there was a commercially available perfusion phantom for the validation study of the ARTIS icono-Siemens Cone Beam CT at the UMCG. The study concluded that the most appropriate phantom for the validation study was the phantom used by Boese et al [42]. Other phantoms that were potentially interesting were the phantoms made by Driscoll et al. [38] (see section 3.2.2), Mathys et al.[43] and Suzuki et al. [44].

A. Boese et al. [42], developed a C-arm CT brain perfusion phantom and evaluated its performance. The phantom consists of four feeding arteries which are divided into sixteen sub-branches, leading into the sinter board (high-density polyethylene micro-porous sinter board), which simulates the capillary tissue (figure 3.4a). The porosity size of the board is equivalent to the diameter of brain capillaries. In this study, CT perfusion maps of the sintered board were computed and compared for CT and C-arm CT systems. Flow and contrast medium parameters were altered and a perfusion deficit was simulated by clamping one of the arterial input tubes. The CBV and CBF maps had a strong relationship and were reproducible. Quantitative perfusion measurements with C-arm CT were not possible due to under-sampling of the time-intensity curves. The phantom set-up was not validated, e.g. the CBV and CBF were not related to the actual flow measured with a flow sensor.

Mathys et al. [43], developed a brain perfusion phantom to investigate inter scanner comparability of CT brain perfusion parameters. The phantom is designed as a discoid with centrifugally directed flow through 1.5 mm-sized polyoxymethylene (POM) globes which simulate brain parenchyma. Figure 3.4b shows the phantom, which consists of two rings (red arrows) with the POM globes in between (black asterisk), water/contrast flows in the inner ring via four arteries (blue arrows), small ducts (black arrows) in this inner ring lead to the brain parenchyma. The water/contrast flows out via 4 draining arteries (green arrows). With the phantom reproducible simulations of cerebral perfusion were achieved to examine the differences in cerebral blood volume (CBV) and cerebral blood flow (CBF) between CT scanners.

The phantom developed by Suzuki et al. [44], consists of a hollow-fiber hemodializer cartridge surrounded by a syringe-shaped body to simulate the absorption of X-rays by the brain. Figure 3.4c shows the phantom and a schematic cross section which shows the locations of the ROIs for analyses. With this phantom the aim was to investigate quantitative accuracy of CT perfusion under low dose conditions. In this research problems with clinical software and recognition of the phantom as a brain were experienced. The hollow spaces in the phantom resulted in high-contrast images because the space ratio (ml/100gr) of the dialyzer was much greater than the clinical range of CBVs, as a result the CBV and CBF values did not resemble clinical values.

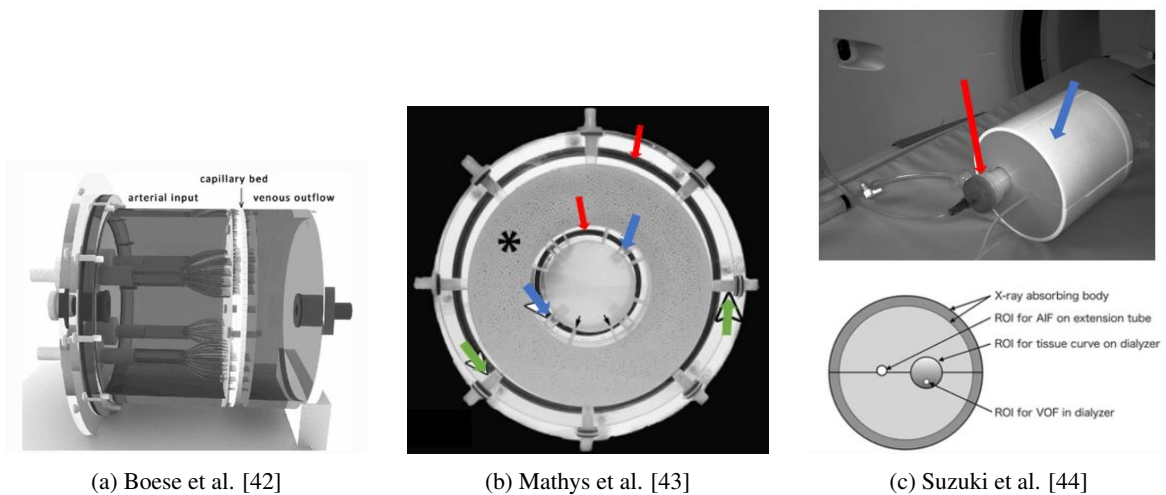


Fig. 3.4 State of the art brain perfusion phantoms

(a) Phantom by Boese et al. four feeding arteries splitting up into sixteen sub-branches feeding into a sinter board (simulating capillary tissue). (b) Phantom by Mathys et al. A discoid with two rings (red arrows) filled with polyoxymethylene globes (black asterisk) which simulate the brain tissue, four feeding arteries (blue arrows), small ducts into tissue compartment (black arrows) and four draining arteries (green arrows). (c) Phantom by Suzuki et al. hollow-fiber hemodializer cartridge (red arrow) surrounded by syringe-shaped body to simulate the X-ray absorption of the brain. The cross section shows the locations of the ROIs for analyses.

From this past research, it was learned that it should be possible to simulate microcirculation perfusion. A. Boese et al., and Mathys et al., succeeded in making reproducible models for the visualization of cerebral perfusion. However, the CBV and CBF have not been related to the actual flow in the phantom set-up. This is an important step in the validation of the results, and something that should be eventually aimed for in this research.

3.3 Phantom requirements

With the information that gathered during the market research, the requirements are drawn up. The requirements are split up into five categories: (1) requirements regarding the anatomy/ morphology of the phantom, (2) the physiology, (3) the pathophysiology, (4) imaging and analyses, and (5) overall requirements of the phantom. The requirements per category are explained in the sections below. An overview of the requirements is shown in the table in appendix A.

3.3.1 Anatomy/morphology

The phantom should simulate certain structures (anatomy) and their shape (morphology).

- The phantom should simulate both the macrovasculature and microvasculature of the lower extremities

The macrovasculature is represented by the a. Tibialis posterior with a diameter of 0.22 cm [45], the a. Cerebralis anterior (brain) is 0.24 cm [46]. The incoming flow tube should resemble the a. Tibialis posterior and have a diameter of 0.22 cm. The incoming flow tube and outgoing flow should be visible in the field of view in order to compute an arterial input and venous outflow function.

The macrovasculature branches into the microvasculature and the diameter of the vessels gradually changes from 0.22 cm to 5-100 micrometers (arterioles) to 5-10 micrometers (cappillaries) [47]. In the phantom, the macrovasculature should branch into the microvasculature, to slow down the flow and get to an even distribution of fluid into the microvasculature compartment. The incoming flow tube should be 0.22 cm and the sizes of the branches should be that size or smaller.

The phantom should simulate the (perfusion of) target tissue, in this case, muscle. The attenuation coefficients of the used material should be in the same range as the attenuation of muscle (-29 Hounsfield units (HU) to 150 HU [48]). The target region should be designed in such a way that the time-intensity curves (TICs) of the contrast flow through the target region are in the same ranges as the ones in the lower extremities. The phantom should have a part that simulates bone (the Tibia), this part should have the same attenuation coefficient as bone (250 - 1000HU) [49] and the size (diameter) of the Tibia (2 cm) [50].

The phantom should be compatible with the clinical analyses software of the CT perfusion scanner in the university hospital of Groningen, Syngo.Via, in order to be able to study brain perfusion imaging with the phantom set-up.

- The phantom should be designed to simulate a 2D and 3D situation and investigate if a 2D scan leads to different results regarding perfusion compared to a 3D scan. The phantom should have different configurations, namely: completely, partly and no overlapping structures in one plane.

3.3.2 Physiology

- The phantom should be able to simulate blood flow in the macrovasculature in the same ranges as in the lower extremities.

In the a. Tibialis Posterior the blood flow is 30 mL/min, and the blood pressure ~ 95 mmHg [51].

In the brain the total cerebral blood flow is 700 mL/min, this is the sum of the blood flow of all the cerebral arteries [52]. Blood flow values for individual cerebral arteries are for example: 257 mL/min in the carotic artery, 110 mL/min in the anterior cerebral artery and 146 mL/min in the middle cerebral artery [52]. In the analysis we are interested in the cerebral blood flow (CBF), cerebral blood volume (CBV) and mean transit time (MTT) of the microcirculation of the brain, and getting these values to resemble patient values (the patient values are shown in table 3.1). It is of less importance to get the macrocirculation values of the brain correct.

Based on the blood flow in the lower extremities the lower boundary of the flow range in the phantom should be 30 mL/min, and based on the blood flow in the brain the upper boundary should be 250 mL/min.

Table 3.1 Clinical values of CBV, CBF, time to peak (TTP) and mean transit time (MTT), for healthy patients and the penumbra and core in patients with ischaemic stroke [53]

	Healthy	Penumbra	Core
CBV (ml/100g)	3.8 \pm 0.7	2.15 \pm 0.43	1.12 \pm 0.37
CBF (ml/100g/min)	44.4 \pm 6.5	25.0 \pm 3.82	13.3 \pm 3.75
TTP (seconds)	16 \pm 5.6	26 +- 1.5	36 +- 1.5
MTT (seconds)	4	7 +- 1.5	8 +- 1.5

- The phantom should be able to simulate blood flow in the microvasculature in the same ranges as in the lower extremities and brain.

In the brain, the blood flow is 60 mL/min/100gr in a healthy situation [54]. In the pathological situation the blood flow is 20 mL/min/100gr [54]. In the microcirculation, in the leg, the blood flow velocity is 1.1 +- 1.1 mL/min/100 gr [55].

The time that the contrast is staying in the microvasculature should be comparable to human values. The MTT in the microvasculature ranges from one second in healthy tissue to 30 seconds in pathological situations in the lower extremities (measured in an ROI of 7200 mm²) [56]. In the brain the mean transit time for the healthy and pathological situations is shown in table 3.1.

The blood pressure in the arterioles is ~ 60 mmHg, in the capillaries ~ 25 mmHg, in the venules ~ 15 mmHg, and in the veins ~ 15 -30 mmHg [51]. The goal of the phantom is to produce similar time-intensity curves as in the lower extremities of the human body. Pressure plays a role in the contrast flow velocity, however to achieve the goal it is not necessary to simulate the exact blood pressures as in the human body. Therefore, we do not intend to take these specified pressures exactly into account.

3.3.3 Patho-physiology

The phantom should have one 'healthy' part and one part with a perfusion defect, they should be imaged at the same time to show the differences in the TICs between healthy and diseased tissue. The flow should be adjustable from 0 to 100% with steps of 15%, to simulate different perfusion states. The arrival time of contrast

should be adjustable to 25 % later arrival [57], this percentage is the average increase of arrival time in patients with critical limb ischemia after revascularisation. In case of critical limb ischemia, collaterals will form to take over the vascularisation [58]. The phantom should be able to simulate this.

3.3.4 Imaging and Analyses

With the phantom set-up it should be possible to produce TICs of the macrovasculature perfusion and TICs of the microvasculature perfusion, similar to the ones in the lower extremities and brain as measured in the clinic with C-arm angiography and CT perfusion respectively. Values of interest include the arterial input function (AIF), venous output function, time of arrival (TOA), time to peak (TTP), slope of the curve, maximum value and MTT.

3.3.5 Overall requirements

The phantom set-up should be standardised and reproducible. Furthermore, the phantom set-up should be applicable for imaging with angiography systems, cone beam CT and CT perfusion.

4 | Phantom design and realisation

In this chapter it is described how the requirements and information gathered with the market research are translated to possible design options. The options are compared and the definitive design is chosen. After realisation of the phantom set-up, initial tests on the functioning of the set-up are performed.

4.1 Phantom design

4.1.1 Morphological chart

After drawing up the requirements, possible solutions are thought out. These solutions are visualized in a morphological chart. The morphological chart lists the sub-functions identified in the requirement section and shows the solutions that can perform each sub-function. Figure 4.1 shows the morphological chart. An elaboration on some options described in the morphological chart and options for manufacturing the phantom is given below.

Transition from macrovasculature into the microvasculature

The transition from the macrovasculature into the microvasculature can be designed in different ways. The first option is a design in which the incoming artery branches three times into eight arteries. These arteries lead into the microcirculation compartment. In this way the flow will be slowed down and an even distribution of fluid in the microcirculation is achieved. The other option is a design in which one macrocirculation artery flows *alongside* the microcirculation compartment, small holes/sieves on the border will ensure the fluid to flow into the microcirculation compartment, the fluid that did not flow into the microcirculation compartment flows past and around it to flow out on the other side again.

Microvasculature material

The microvasculature compartment should be filled with a material that simulates tissue perfusion. This material should have the same Hounsfield Unit as muscle/soft tissue, which is between -29 and -150 HU. The flow through the microcirculation compartment should be able to resemble the blood flow through tissue in the lower extremities and the brain; Between 1-60 mL/min/100gr, without sinking of the contrast agent. With the microcirculation compartment, it should be possible to get to the same TICs of the microcirculation in the lower extremities and the brain. The design could be either a capillary phantom or a tissue-filled phantom. In a capillary phantom, the microcirculation is simulated with hollow fibers or straws [34], e.g. the phantom used by Suzuki et al. [44] incorporated a hemodialyzer cartridge to simulate the microcirculation. The diameter, amount, and permeability of the fibers can differ [34]. In tissue-filled phantoms, different types of sponges or particles can be used. Sponge materials can differ in among other things permeability, pore diameter, and porosity. Possible sponge materials to simulate tissue perfusion are cellulose sponges [59] (made from wood

fiber) which have a larger pore size, polyurethane sponges (commonly used in kitchen sponges) [60] which have a smaller pore size and polyethylene [42] that has a very small pore size. Particles used to simulate tissue in perfusion phantoms include plastic beads [43], which hardly take up any water or gel beads where water can diffuse in and out of, similar to trans-capillary fluid exchange in tissue [61].

Simulation of the perfusion defect

The perfusion defect could be simulated by adding a flow control tab behind the microcirculation compartment, this will increase the resistance in the microcirculation compartment and reduce the flow through it. Another option is to add a flow control tab in front of the microcirculation compartment, to simulate a stenosis in the incoming artery, which reduces the flow through the microcirculation compartment. If the design of the flow alongside the microcirculation compartment is chosen, a perfusion defect can either be simulated by making smaller holes between the macro- and microcirculation or by reducing the amount of holes between the macro and microcirculation.

Manufacturing the phantom

3D printing techniques can be used to manufacture the phantom. Depending on the design, different approaches can be taken. The vascular structure could either be directly printed using fused deposition modeling (FDM), stereolithography (SLA) or selective laser sintering (SLS) 3D printing, or a negative mold can be made which can be filled with a material.

In FDM 3D printing a thermoplastic filament (such as acrylonitrile butadiene styrene (ABS) or polylactic acid (PLA)) is melted and extruded through a heated nozzle to build a layer (0.25 mm). The layers are build up until the print is complete. FDM 3D printing can be used for basic proof-of-concept models and low-cost prototyping of simple parts. FDM 3D prints are not completely water proof.[62]

In SLA printing a ultraviolet laser cures photopolymer resin. The laser beam can be focused very precisely and the thin (0.05 mm) layers can give fine details. The print is water-resistant. The technique can be used for functional prototyping and molds.[62]

In SLS a high power laser is used to fuse small particles of polymer powder (nylon is mostly used) into a solid structure. The layer has a thickness of between 0.05 and 0.2 mm. Nylon SLS prints are strong and stiff, and water-, temperature- and light-resistant, they can be used for end-use products. [63]

3D printing can also be used to make a negative mold to shape casting material into the desired design. Silicon can be used as a casting material, it is flexible, durable and water-resistant.





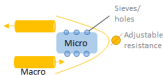



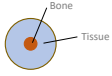

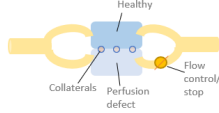
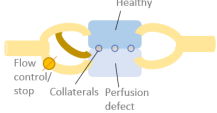
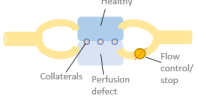
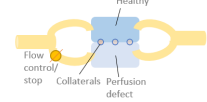
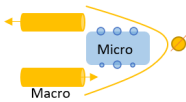
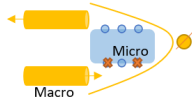
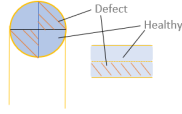

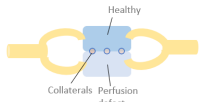
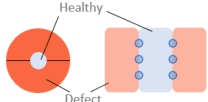
	Solution 1	Solution 2	Solution 3	Solution 4
Macrovasculature Incoming + outgoing artery Arterial input function Brain (0.24 cm)/leg (0.22cm)	Correct diameter of 0.22 cm (a. Tibialis Posterior) Material: ABS 	Standard tube of 0.5 cm diameter 	Phantom input inflow adjustable for variable diameters 	
Flow of macrovasculature to the microvasculature and flow in the microvasculature	Three branches 	Sieves/holes 		
Microvasculature HU muscle: -29 - 150 Time-intensity curve parameters	Capillary phantom Membranes 	Tissue filled phantom Sponge: Polyurethane Cellulose Polyethylene 	Tissue filled phantom Particles: Plastic beads Gel beads 	
Bone Diameter of 2 cm HU bone 250 - 1000	Bone mimicking material in the middle 	Bone material next to phantom 		
Flow macrocirculation Range leg: 30 mL/min Range brain: 250 mL/min	1 pump total range	2 pumps		
Collaterals	Two compartments, "collaterals" in-between 	Two compartments + extra incoming artery 		
Perfusion defect 3 situations	Flow control stop at the outgoing tube 	Flow control stop incoming tube 	Smaller tube/ holes 	Blockage of holes 
2D/3D situation Completely overlapping structures Partly overlapping structures No overlapping structures	Different compartments Quadrants 	Different compartments Changeable modules Variable sizes 		
Healthy & Pathology in one view	2 situations 	3 situations 		
Standardized and reproducible set-up Compatible with C-arm and CT perfusion software Syngo.via	Calibration point	1 fit		

Fig. 4.1 Morphological chart of the phantom set-up, with the sub-functions on the left side and possible solutions per sub-function on the right side

4.1.2 Comparison chart

To generate several prototypes, the possible solutions documented in the morphological chart are combined into three different options. In this section the options are described, appendix B contains the comparison chart of the options.

Option 1

The first option is a flow circuit in which the water and contrast flow sideways along the microcirculation area. The macrocirculation is 3D printed using SLA, for an accurate water-resistant print. The microcirculation consists of a cleaning sponge of polyurethane sponge material. The pore size of this material is slightly larger than the pore size of a usual kitchen sponge but not as large as the cellulose cleaning sponges, to avoid airbubbles but still have some inhomogeneity in the flow pattern because of the pores. The material is easily available and can be cut into any shape. Small holes between the macrocirculation and microcirculation (dark blue and light blue parts in figure 4.2) allow the liquid to flow into and out of the microcirculation area. The liquid that does not flow into the microcirculation area flows directly to the other side of the macrocirculation via a bypass. To simulate a perfusion defect some of the holes can be closed.

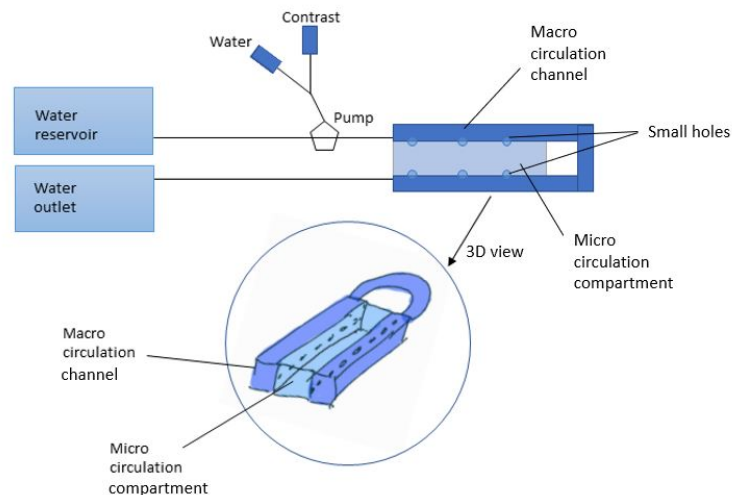


Fig. 4.2 Design option 1: sideways flow

A pump is connected to a water reservoir via a plastic tube to pump water into the phantom. A contrast pump is connected to the tube as well, to give a contrast bolus. The phantom consists of an U-shaped macrocirculation channel where the fluid flows through. The microcirculation compartment is situated in the middle of the U-shaped channel, small holes in the macrocirculation channel allow the fluid to flow into the microcirculation compartment. The other side of the U-shaped macrocirculation channel is connect to a tube which flows out in the water outlet container.

Option 2

The second option is a phantom where the liquid flows into the microcirculation via a macrocirculation simulation of 3x3 branches (figure 4.3). The microcirculation consists of 3 changeable modules which can be filled with a material of choice. The macrocirculation is made of Ecoflex™ material (silicone), this is done by first making a 3D printed negative mold of the branches. A perfusion defect can be simulated by closing off one of the branches. A funnel at the end of the microcirculation compartments collects the outgoing fluid.

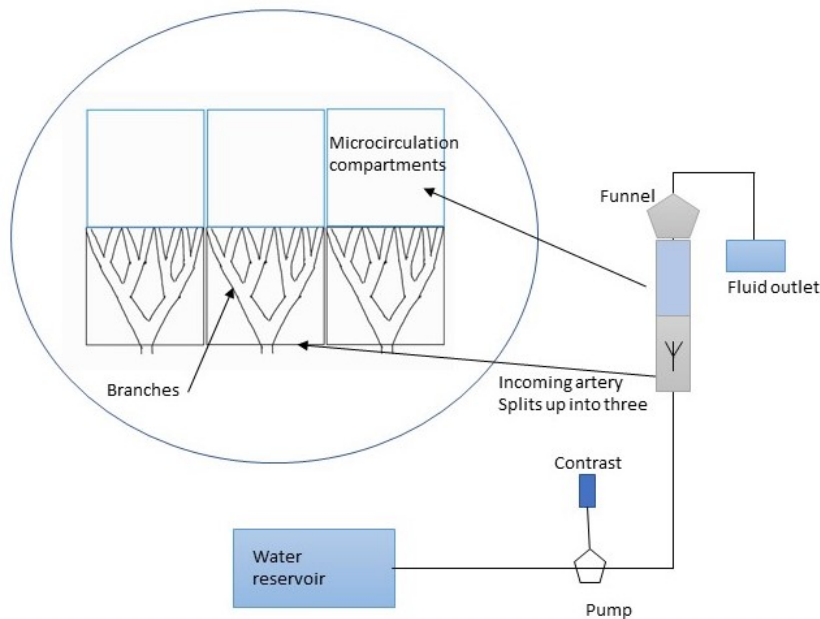


Fig. 4.3 Design option 2: silicon vessel structure of 3x3 branches

A pump is connected to a water reservoir via a plastic tube to pump water into the phantom. A contrast pump is connected to the tube as well, to give a contrast bolus. The incoming artery splits up into three branches, which each branch three times and result into 8 incoming arteries. Each of the three branches is connected to a microcirculation compartment, which can be filled with a material of choice. A funnel collects the outgoing fluid. A perfusion defect can be simulated by closing off one of the branches.

Option 3

The third option consists of one incoming artery which branches 3 times and leads into two microcirculation compartments (figure 4.4). A perfusion defect can be simulated per compartment by adjusting the resistance of the outgoing artery. A dividing wall with or without holes enables the simulation of collaterals. The macrocirculation branches are 3D printed using the SLA printing technique with photopolymer resin material. The microcirculation compartments can be filled with any material.

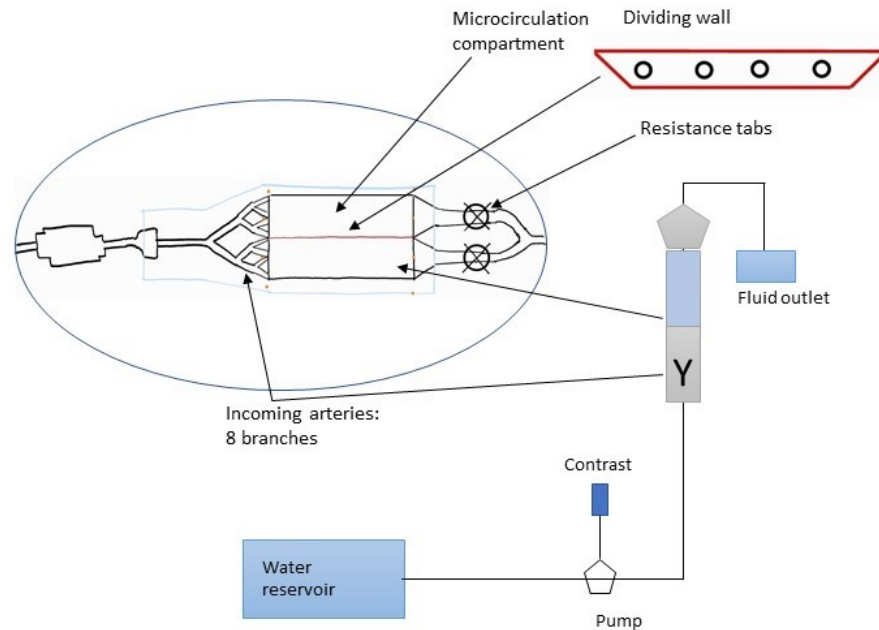


Fig. 4.4 Design option 3: 3D printed vessel structure of 1x3 branches flowing into a microcirculation compartment with dividing wall

A pump is connected to a water reservoir via a plastic tube to pump water into the phantom. A contrast pump is connected to the tube as well, to give a contrast bolus. The incoming artery branches 3 times into 8 incoming arteries which enter the microcirculation compartment. A dividing wall, with or without holes, separates the microcirculation compartment into two compartments. Two resistance tabs at the end of the compartments regulate the flow through the compartment. By closing off one of them, a perfusion defect can be simulated.

4.1.3 Final design and realisation of the phantom set-up

Phantom

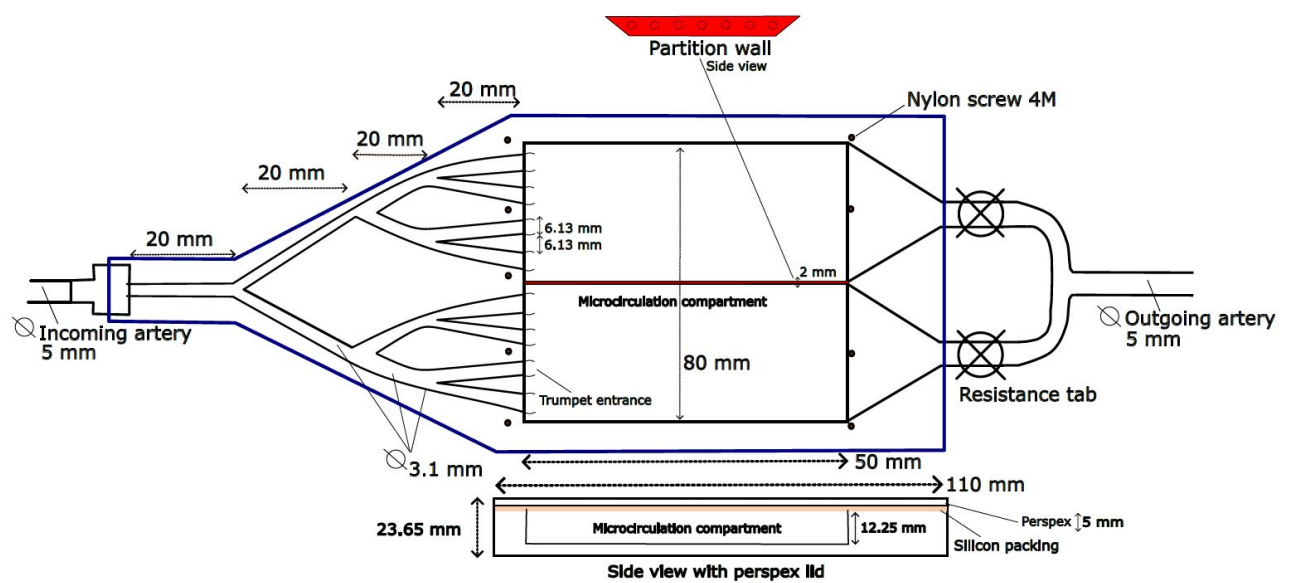
The final design of the phantom is based on option 3. The phantom meets most of the requirements and the production process is more controllable than options 1 and 2. The design is shown in figure 4.5. The phantom is 3D printed using a stereolithography printer with transparent resin material.

The contrast agent and water enter the phantom via one incoming tube with a (standard) tube diameter of 5 mm. This tube branches three times which results in 8 incoming tubes. All branches have the same diameter of 3.1mm, a diameter of 2.5 - 2 mm based on the Arteria tibialis posterior and a decreasing diameter over the branches would have been preferred, however, a larger diameter was required to be able to open the 'arteries' after the printing process. This is not expected to be a problem since the eight incoming tubes with the given diameter will suffice to create an even distribution of contrast agents in the microcirculation material.

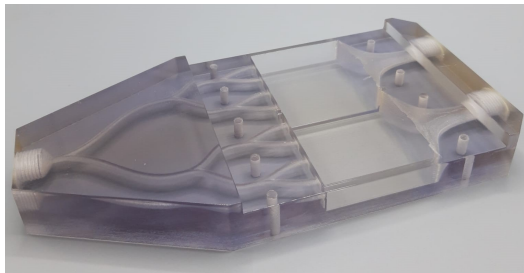
The microcirculation compartment can be filled with a filling material of choice. The compartment can be closed off with a partition wall to create two compartments. The partition wall can be changed for a

partition wall with holes, the holes can be used to simulate collaterals. The compartment is easily accessible because of the lid on top of it. In this way, the filling material can be changed and the partition wall can be added or taken out. The lid and partition wall both have a silicon packing material to prevent water leakage, they are screwed on top of the phantom with nine nylon screws. The microcirculation compartments lead into two funnels, which collect the outgoing fluids into an outgoing tube. Both outgoing tubes are connected to a flow regulator. In this way, the resistance in both microcirculation compartments can be regulated separately.

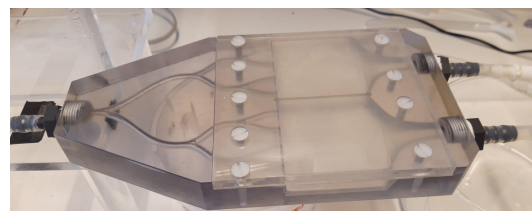
The phantom has a height of 23.65mm. The microcirculation compartment has a height of 12.25mm. The relatively small height makes it easy to print the phantom.



(a) Schematic overview of the phantom design



(b) 3-D print of the phantom



(c) 3-D print of the phantom with the lid and tubes connected

Fig. 4.5 Phantom design

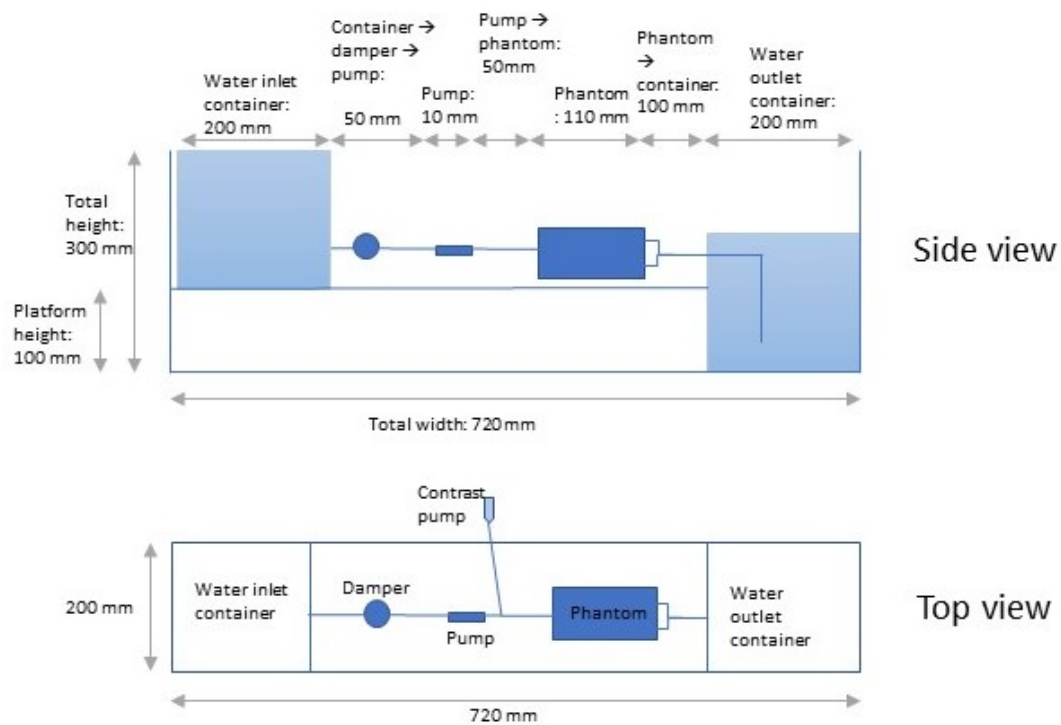
(a) Shows the schematic overview of the phantom design. The top view of the entire phantom and the side view of the microcirculation part of the phantom are shown. The sizes of the parts are noted. (b) Shows the 3D print of the phantom. (c) Shows the assembly of the 3D printed phantom. The lid with silicon packing is screwed on top of the phantom and tubes are connected to the ends. The microcirculation compartment is empty but can be filled with a material of choice.

Phantom set-up

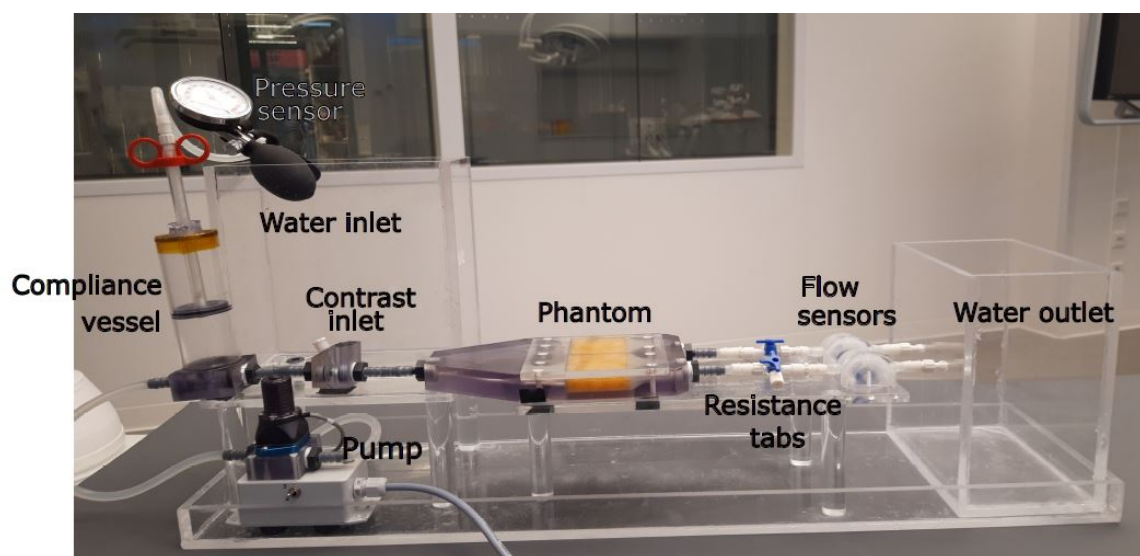
The schematic overview and realisation of the phantom setup are shown in figure 4.6. The set-up is placed on a platform with a total length of 720 mm. The water reservoir is placed on a platform to create a height difference for the water flow.

A pump (RS Pro Micropump R400BL-M) is placed next to the water reservoir to pump the water into the phantom. This is a self-priming conical pump, which works by the peristalsis principle. The advantage of this principle is that the pump is valveless and the direction of the flow can be reversed. The pump has a maximum operating pressure is 2.0 Bar (29psi). Since the pump does not generate a stable flow, a compliance 'vessel' is connected to the output. In this way, a constant flow can be realised.

After the compliance vessel, the tube from the water reservoir is connected to the tube from the contrast pump. The resulting tube leads into the phantom, which is placed in the area between the outgoing and ingoing water reservoirs. The two outgoing tubes of the phantom are both connected to flow sensors and flow regulators. The flow sensors are Bio-Tech FCH-m-PP-LC 155374 low flow sensors. These sensors have a flow range of 0.015-0.8 L/min and have the advantage that they are transparent, and therefore offer the possibility to see when air bubbles get stuck in the sensor. Thereafter, the tubes lead into a reservoir to collect the outgoing fluid.



(a) Schematic overview of phantom set-up, side view and top view



(b) Phantom set-up realisation side-view

Fig. 4.6 Design and realisation of the phantom and set-up

4.2 Initial testing of the phantom set-up

Before performing imaging experiments with the phantom setup, three initial tests are performed. The flow sensors are calibrated, the pumping output is tested and the effect of a decreasing water level on the flow velocity is investigated. In this section, the experiments are described and the results are discussed.

4.2.1 Flow sensor calibration

Goal The goal of these tests is to determine the conversion factor of the flow sensors.

Method A schematic overview of the set-up is shown in figure 4.7. A 10-liter water cylinder was connected to a pump which added water to the cylinder if the water level fell below 8 liters, a sensor kept track of the water level. The flow sensors were connected in series with each other and the water cylinder. The flow sensors were first placed 40 cm below the water cylinder (experiment set 1) and thereafter 10 cm below the water cylinder (experiment set 2). During 30 seconds the volume output was measured and the output frequency of the flow sensors (pulses per second) was shown on an oscilloscope and written down. In set 1 the experiment was performed 10 times in a row (set 1a), thereafter the set-up was reconnected and the experiment was conducted another 5 times (set 1b). This protocol was repeated during set 2 with the water cylinder at a height difference of 10 centimeters. With the volume per 30 seconds and the average frequency of the flow sensor, the conversion factor of the flow sensor in pulses per liter could be calculated.

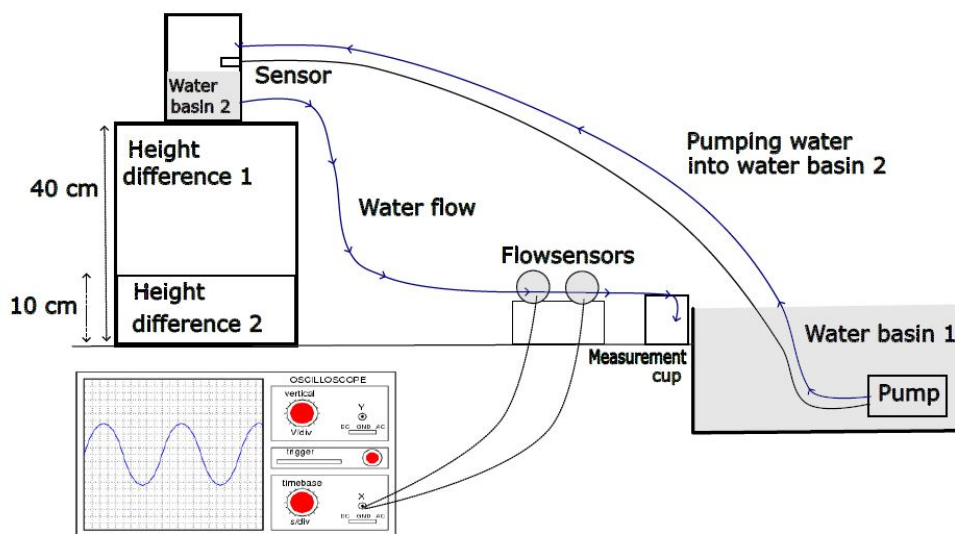


Fig. 4.7 Flow sensor calibration set-up

A pump pumps water out of water basin 1 into water basin 2, if the sensor detects a water level below a certain height. Water flows from water basin 2, through the flow sensors into a measurement cup. The frequency (amount of pulses per second) of the flow sensors is shown on an oscilloscope. Water basin 2 can be placed on two different heights for different flow velocities.

Results Table 4.1 shows the result of the experiment. The conversion factor (i/L) in set 1a and set 1b is similar, there is a small difference, but not a significant one. The difference between set 1 and set 2 is larger: about one thousand pulses per liter for each measurement. Which results in a difference of 1mL per minute. When the

flow is lower the conversion factor seems to be lower as well.

Table 4.1 Flow sensor calibration.

On the left side the four different experiment sets are shown (set 1a and b, and set 2a and b, in set 1 the flow velocity was higher). The average frequency and standard deviation (std) per sensor, per set per sensor is given and the average volume in 30 seconds and standard deviation, per set per sensor is given. With these values the average conversion factor in pulses per liter is calculated.

		Avg. Frequency (Hz)	Std (mHz)	Avg. Volume (mL/30 seconds)	Std (mL)	Avg. i/L
Set 1a	Sensor 1	17.16	135	46.25	0.54	11111
	Sensor 2	16.30	202	46.25	0.54	10790
Set 1b	Sensor 1	16.89	105	46	0	11034
	Sensor 2	16.50	130	46	0	10793
Set 2a	Sensor 1	9.80	106	29	0	10199
	Sensor 2	9.44	124	29	0	9813
Set 2b	Sensor 1	9.27	106	29	0	9660
	Sensor 2	9.08	125	29	0	9417

4.2.2 Testing the pumping output

Goal The goal of these tests is to investigate what the minimum and maximum volume output of the pump is and if the volume output increases linearly when the pumping rate is increased.

Hypothesis We expect to see a linear relationship between the pumping rate and the flow rate.

Method The pump can be set on different pumping rate settings, from zero dots to five dots (see figure 4.8). It is not specified to what flow velocity these dots correspond. The minimum and maximum output of the pump is investigated by measuring the volume output behind one microcirculation compartment of the phantom for 30 seconds, while both microcirculation compartments are open. The volume output when the pumping rate of the pump is set on 0.5 dot, 1 dot, 1.5 dots and 2 dots is also tested. Each measurement is performed three times in a row.

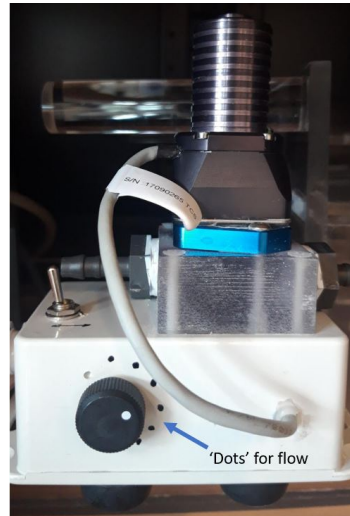


Fig. 4.8 The pump used in the set-up. The further the wheel is turned clockwise, thus the more 'dots,' the higher the pumping rate and flow output.

Results The minimal setting of the pump is one 'quarter' of the first dot, a slower setting is not possible. The maximum setting of the pump in combination with our set-up is 3 dots, a higher setting results in a pressure in the phantom set-up which is too high and causes leaking. The volume output for one quarter of the first dot, up till the third dot is measured and shown in figure 4.9 The minimal flow velocity achieved with the minimal pumping rate was 104 mL/min, the maximal flow rate was 280 mL/min.

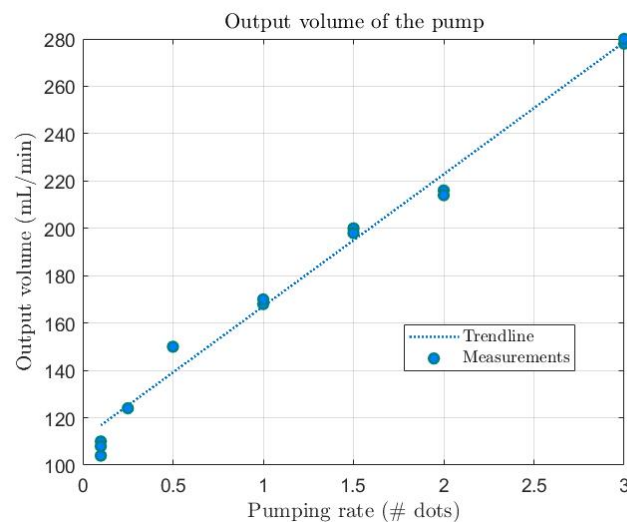


Fig. 4.9 Volume output in mL/min behind one compartment for different pump settings

4.2.3 Testing the effect of a decreasing water level

Goal The goal of these tests is to investigate what the effect of the water level in the first water tank is on the flow velocity of the water in the phantom set-up.

Hypothesis We expect a decreasing flow velocity when the water level decreases.

Method We start with a full water tank, set the pump on 1.5 dots and write down the frequency of the flow sensor behind the right microcirculation compartment every 60 seconds until the water tank is empty. With the flow sensor conversion factor (determined in section 4.2.1), the frequency of the flow sensor is converted to a flow rate.

Results The results are shown in figure 4.10. The total measurement took 900 seconds.

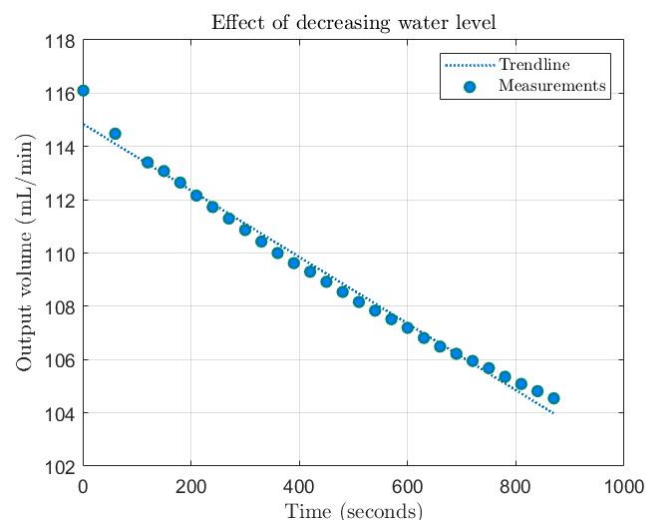


Fig. 4.10 Effect of decreasing water level (over time) on the flow velocity

4.2.4 Conclusions and discussion of initial tests

Flow sensor calibration

There are several factors affecting the measurements. The flow sensors are affected by air bubbles, these can get stuck inside the sensor and influence the number of rotations, thus the frequency that is read out. It was tried to reduce this as much as possible by keeping a close eye on the sensors and taking them out when they were discovered. The position of the flow sensors could have affected the measurements as well. The flow sensor were positioned on a stand. They were however not fixed, displacements can affect the sensor output.

A difference in 1000 pulses/L in the conversion factor leads to a volume difference of about 1 mL/min (this is based on a frequency of 16Hz), when the set-up is used for quantitative measurements the flow calibration needs to be improved. In the experiments, the conversion factor decreases when the flow decreases, it is recommended to repeat the experiment with different flow velocities and plot the conversion factor against the flow velocity, to see if there indeed is a different kind of relation between the two. The flow range of our measurements should be between 30 mL/min and 250 mL/min (based on the flow velocities in the lower extremities and brain [51] [52]), it is recommended to repeat the flow calibration experiments for flow velocities in this range as well. The manufacturer recommends using a conversion factor of 10.500 for a flow of 0.015-0.8 L/min. This factor is in line with our findings during set 1. We proceed with a conversion factor of 11.050 for sensor 1 and 10.790 for sensor 2, based on the measurements with the higher flow and keep the conversion factor the same for each experiment.

Pumping output

From figure 4.9 it can be concluded that the three measurements in a row lead to a consistent result, so once the pump is set on a certain dot, the power output is fixed. The output volume increases linearly when the amount of dots is increased. We are interested in a flow between 30 mL/min (leg) and 250 mL/min (brain) [51] [52]. With this phantom set-up the flow rate of the brain can be achieved, however the flow rate is too high to simulate the flow in the leg. For the first C-arm CT experiments this should not be a problem, as the reproducibility of the set-up is tested and the effect of a perfusion defect, flow velocity, imaging system and protocol on the time-intensity curves is investigated. When the phantom measurements are compared to patient measurements, the flow difference needs to be taken into account. At the moment that the flow needs to resemble the physiological flow, a different pump should be found or the phantom set-up should be adjusted.

Effect of decreasing water level

When the water level decreases the frequency of the flow sensor decreases, hence the flow velocity decreases. From this experiment it can be concluded that it is important to keep the water level in the tank stable, in order to generate a stable flow velocity.

All in all, the phantom set-up can be used for the first set of experiments. In the future the correct conversion factor for the flow sensors needs to be further explored and it needs to be investigated how lower flow velocities can be achieved in the set-up.

5 | Testing the phantom: studying 2- dimensional phantom perfusion imaging with C-arm angiography

In order to investigate the behaviour of the phantom we conducted 2-D perfusion angiography measurements at two different imaging systems: the SIEMENS Artis Pheno system at the Techmed Centre of the University of Twente in an experimental setting (from now on called 'System 1') and the GE Healthcare Discovery IGS740 system at Medisch Spectrum Twente (MST) in a clinical setting (from now on called 'System 2').

The goal of the experiments at system 1 was to address the question if it would be possible to obtain a realistically shaped time-intensity curve (TIC) with the phantom. Thereafter, the reproducibility of the phantom was tested. Furthermore, the effect of adjusting the resistance of one of the compartments, to simulate a perfusion defect, was tested.

The goal of the experiments at system 2 was to compare the results obtained at system 1 and determine what the effect of the imaging protocols used in the clinic was on the TICs. In this way we can find out how different imaging systems and different imaging protocols influence the results.

With the results of both experiments we can judge the suitability of the phantom and if improvements are required. In any case, small adjustments can be made in between experiments (entering the test and retesting phase of the design circle (see chapter 3.1). Identification of the limitations of the current phantom set-up can introduce the start of the next iteration of the design circle (see chapter 3.1), and ultimately lead to a phantom set-up complying with all the requirements. In this chapter the analyses method of the 2-D phantom perfusion measurements is explained, thereafter the different experiments are described and a conclusion and discussion is drawn up.

5.1 Analyses method: semi-automated two-dimensional perfusion analyses in MATLAB

With the perfusion measurements, we aim to make TICs and extract perfusion measures from them (see chapter 2.3). In this research, MATLAB is used to analyze the two-dimensional angiography images and compute the TICs. A semi-automated method is written and the reproducibility is tested.

5.1.1 The analyses protocol

First, the images are loaded into MATLAB. Then, the squeeze function is used to remove the 4th (empty) dimension of the DICOM file to be able to use the file in MATLAB. A function is created to select the ROIs in a standardized way: to get the same ROIs between different measurements and (angiography) imaging systems. With this function, the image is enhanced and the rotational angle is determined. The next function rotates all frames if necessary. Figure 5.1 shows the resulting ROIs of the function for ROI selection. Thereafter, the average values of the ROIs are calculated. An optional function re-scales the averages to get to a value between 0 and 1, however, when using this function the intensity values between measurements cannot be compared anymore, thus it should only be used to compare the values within one measurement. The last two functions compute the TICs and their values ((TOA), Time To Peak (TTP), Mean Transit Time (MTT), Slope of the curve (SOC) and the maximum intensity (MAX)). The MATLAB functions are described in appendix C.

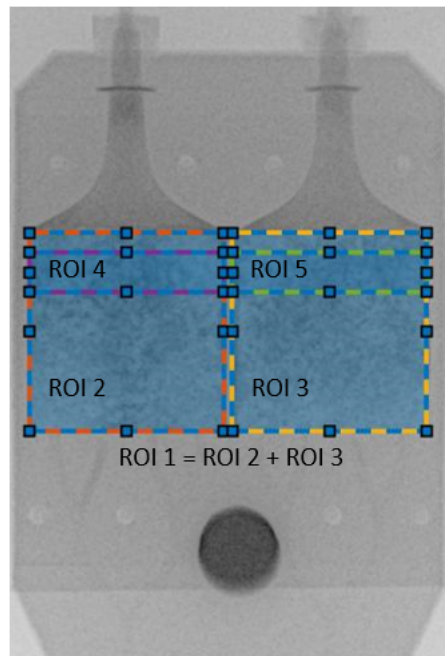


Fig. 5.1 The ROIs of the phantom

Figure 5.2 shows the TICs computed of one measurement with the data obtained from the function that computes the average of the ROIs (figure 5.2a) and with the data obtained with the function that re-scales the average of the ROIs (figure 5.2b). During the measurements the un-scaled values will be used, however, the values will be inverted. In this way the TICs will get the regular shape; a peak at maximum intensity instead of a dip, shown in figure 5.2c. The x-axis shows the time in seconds the y-axis shows the pixel intensity, the un-scaled pixel intensity is a uint16 variable, and the range of a 16-bit intensity image is [0, 65535].

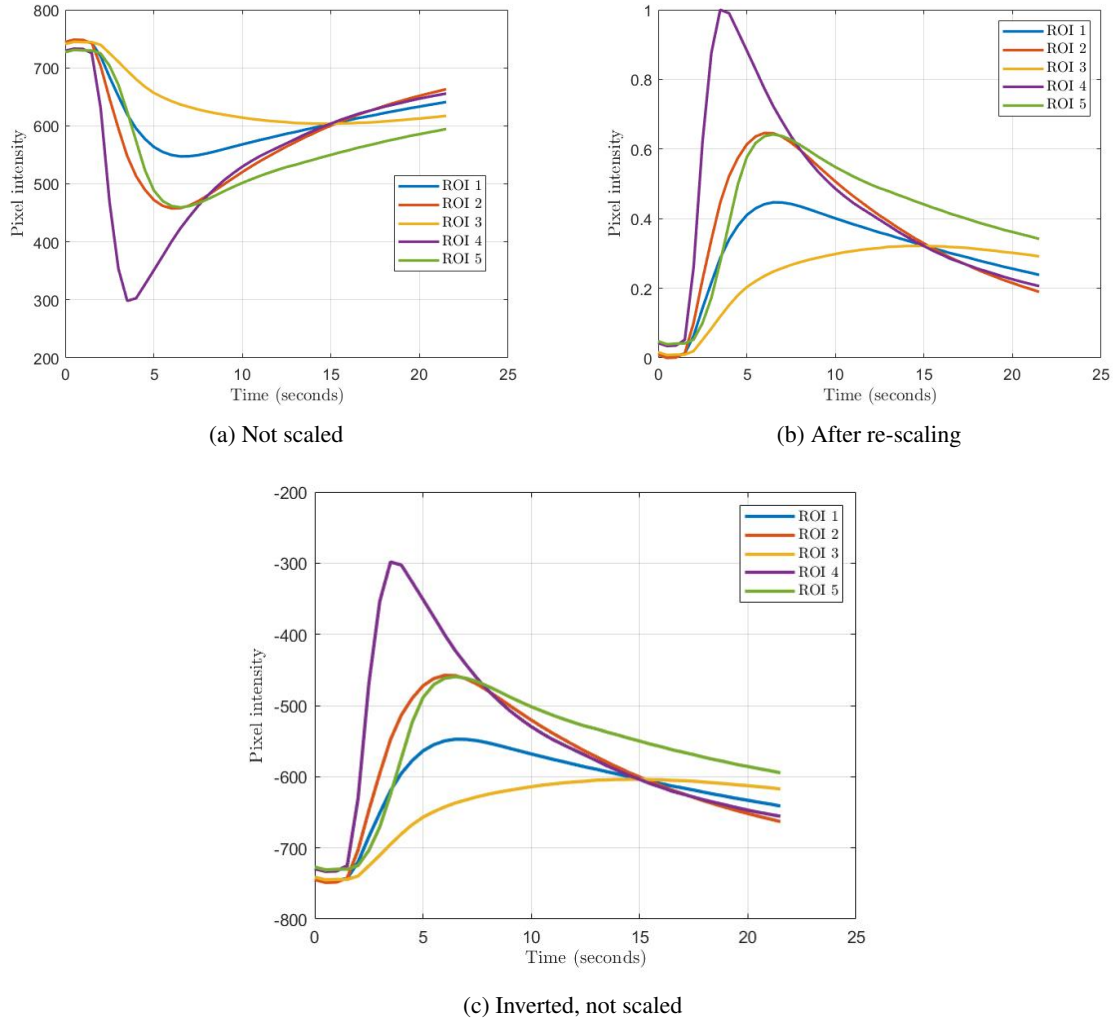


Fig. 5.2 Showing different analyses options: TICs of the same measurement for the five different ROIs
(a) not scaled (b) after re-scaling (c) inverted, not scaled

5.1.2 Reproducibility of the analysing method

To test the reproducibility of the analyses method, the analysis was performed ten consecutive times on measurement 1 from the measurement at the MST. This measurement was done using the standard angiography imaging protocol (30 seconds, 2 frames per second (fps), tube current of 71 mA, tube Voltage of 66 kV). The values TOA, TTP, MTT, SOC, and MAX, were computed for each ROI. The average and (percentage of the) standard deviation of these values over 10 analyses' was computed.

For ROIs 1, 2, 4, and 5 all the measurements have a standard deviation that does not exceed 1%. For ROI 3 the standard deviation is however slightly higher for the TTP and the SOC, with a standard deviation of 3.13 and 2.6 percent. ROI 3 is the entire right compartment, the TTP is calculated by taking the time until the maximum of the curve is reached minus the time of arrival. The ROI selection is based on a manual selection of three points: first two points to calculate the angle, then one point that is used to draw the rectangles in the

correct positions. If the angle is slightly off, ROI 1, 2, and 3 can overlap one of the incoming arteries. This will result in a decreased TOA and TTP and an increased slope of the curve and maximum, as the contrast in the incoming arteries have a higher intensity than the contrast in the microcirculation compartment. In this case, there was one measurement with a different TTP in ROI3, as can be seen in the box-plot (figure 5.3b), resulting in a deviant slope as well, as can be seen in the box-plot in figure 5.3a. The bottom and top of the boxplots are the 25th and 75th percentiles of the measurements. The distance between the bottom and top is the interquartile range. A measurement is considered an outlier when the value is more than 1.5 times the interquartile range away from the bottom or top of the box. Overall, it can be concluded that the differences between analyses' are very small and the semi-automatic analysing method is reliable.

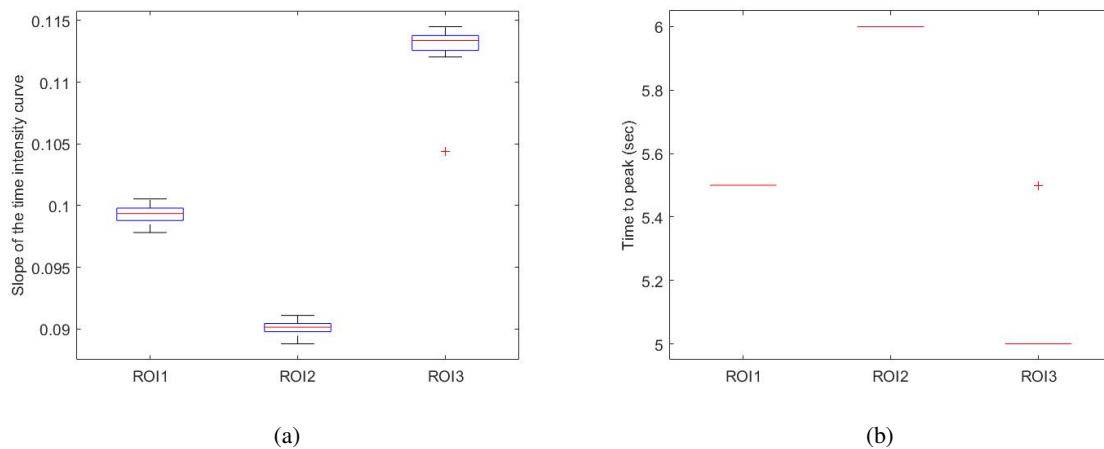


Fig. 5.3 Studying the reproducibility of the analysing method: Box-plots of the slope and time to peak (TTP) of the curve in ROI 1-3 computed in 10 measurements
(a) Slope (b) TTP

5.2 Proof of concept and comparison with clinical values

Goal The aim of the first experiment is to test if realistically shaped TICs can be obtained with the current phantom set-up. These TICs will be compared to TICs of critical limb ischaemia (CLI) patients.

Method To simulate the blood flow in the lower extremities (30 mL/min [51]), the lowest flow setting was used. The obtained TICs were compared to TICs obtained in patient's lower extremities, made with the same imaging system and protocol (system 2).

Hypothesis It is expected that TICs with the same characteristic shape (as described in section 2.3), but with lower intensities, are obtained with the phantom, compared to patient's TICs. Lower intensities are due to the tissue thickness difference between the phantom and patients.

Results Figure 5.4a shows the TICs of the phantom. Figure 5.4b shows the TICs of an area of the foot of an LEAD patient. The shapes of the curves are similar, however the TTP is longer in the TIC of the foot of the patient. (20 seconds in the foot vs 2.5 seconds in the small ROIs (4 and 5) and 6 seconds in the large ROIs (1, 2 and 3) of the phantom).

Discussion The TTP in the TICs of the patient is longer because of three reasons. The first reason is the size of the region of interest, which was larger in the TICs of the patient (4 cm² (ROI 4 phantom) and 20 cm² (ROI 2 phantoms) vs 72 cm² (ROI 5 patient) and 88 cm² (ROI 4 patient)), a larger ROI will lead to a longer TTP.

The second reason is the location of the ROI, in an ROI that is situated further away from the incoming artery, the flow velocity will be lower, therefore the TTP will be longer. The third reason is that the flow velocity in the incoming arteries was too high to correctly simulate the blood flow in the lower extremities, a lower flow velocity will result in a longer TTP. This was however not possible with the current set-up (limited by the used pump which could not generate a lower flow), a lower flow could be achieved by adding a tap to the phantom to release part of the volume.

Conclusion The phantom set-up is able to generate realistically shaped TICs. To make them more similar to TICs from patients, the flow needs to be reduced and the phantom size needs to be enlarged, to enlarge the ROIs.

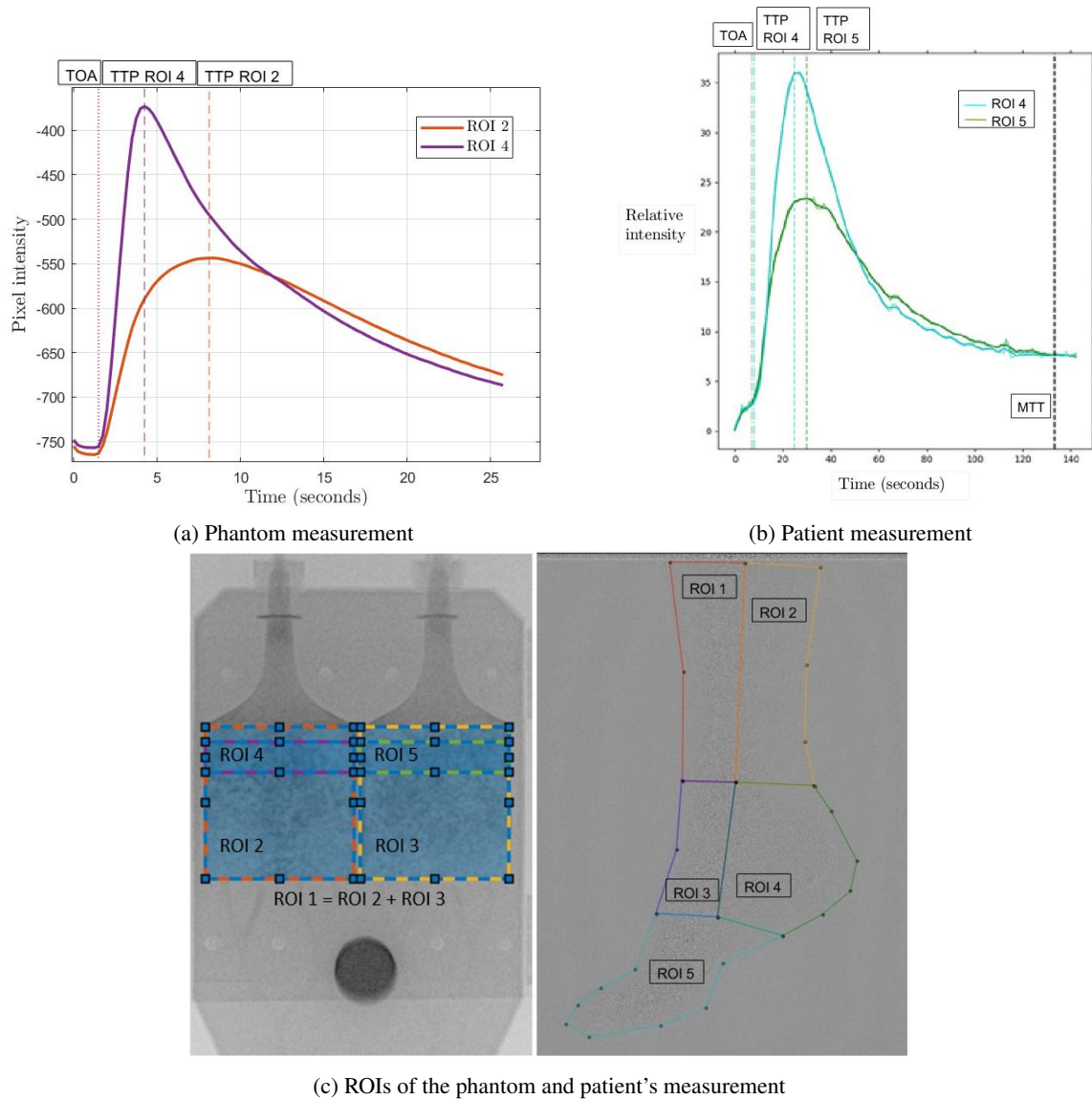


Fig. 5.4 Comparison of the phantom measurements with clinical values: time-intensity curves (TICs) and region of interests (ROIs) of the phantom and the foot of a patient, using system 2

In the TICs in (a) and (b) the time of arrival (TOA) and time to peak (TTP) for different regions of interest (ROI) in the phantom and the foot of the patient are shown. The mean transit time (MTT) for the patient measurement is also given. (c) Shows the ROIs of the phantom and the patient. In the phantom, ROI 2 is 20 cm² and ROI 4 is 4 cm². In the patient's measurement ROI 4 is 88 cm² and ROI 5 is 72 cm².

5.3 Reproducibility of the phantom set-up

Goal The aim of the second experiment was to determine the reproducibility of the phantom set-up. In other words, will the set-up give consistent results while using the same settings.

Method Six measurements were performed, using system 2. In all measurements the same flow velocity was used, while both phantom compartments were fully open. The distribution of the TIC values of the six measurements per ROI is shown in boxplots. The bottom and top of the boxplots are the 25th and 75th percentiles

of the measurements. The distance between the bottom and top is the interquartile range. A measurement is considered an outlier when the value is more than 1.5 times the interquartile range away from the bottom or top of the box.

Hypothesis We expect the TICs to have the same shape and same TIC values: TOA, TTP and slope of the curve.

Results Figure 5.5 shows the TICs of ROI 1 of the six measurements at system 2. The six measurements result in the same TIC within each ROI. ROI 1, ROI 2 and ROI 4 show reproducible results with maximum standard deviations of the time intensity values of 4.4% (TOA), 1.7% TTP and 3.3% (slope). ROI 3 and ROI 5 have one outlier, resulting in a maximum standard deviation in ROI 5 of 16.95 % (TOA). The TICs of ROI 1, ROI 2 and ROI 3 are the same. The TIC of ROI 4 and ROI 5 are different. Figure 5.6 shows the boxplots of the TOA, TTP and slope per ROI.

Discussion The TIC of measurement 1 differs the most in all measurements. Especially in ROI 5 measurement 1 has a different course, this outlier is clearly visible in figure 5.6.

ROI 1, ROI 2 and ROI 3 were expected to have the same TICs, as the contrast should arrive at the same time in both compartments and leave the compartments at the same time as well. This was also the case.

It was expected that ROI 4 and ROI 5 were similar as well, this was however not the case. These ROIs are smaller than ROI 1, ROI 2 and ROI 3, and differences in the sponge material (the size of the air bubbles and thickness of the sponge, which is cut by hand) seem to have an effect on the TIC values. This problem might be overcome by using a cutting machine to get to the same thickness of the sponges or use a different, more consistent material. ROI 4 and ROI 5 are not the same ROIs 4 and ROIs 5 as used in the other experiments, as the phantom was positioned the other way around. ROI 4 and ROI 5 are now positioned on the far end of the contrast inlet, therefore, the effect of the differences between the sponges is expected to be bigger when the contrast has travelled further.

Conclusion When repeating the same measurement the TICs of the phantom are close to uniform. All in all, we might say that the phantom measurements are reproducible during one set of measurements. In the future it should be investigated if the results are the same when the measurements are repeated after the phantom set-up is disassembled and assembled again.

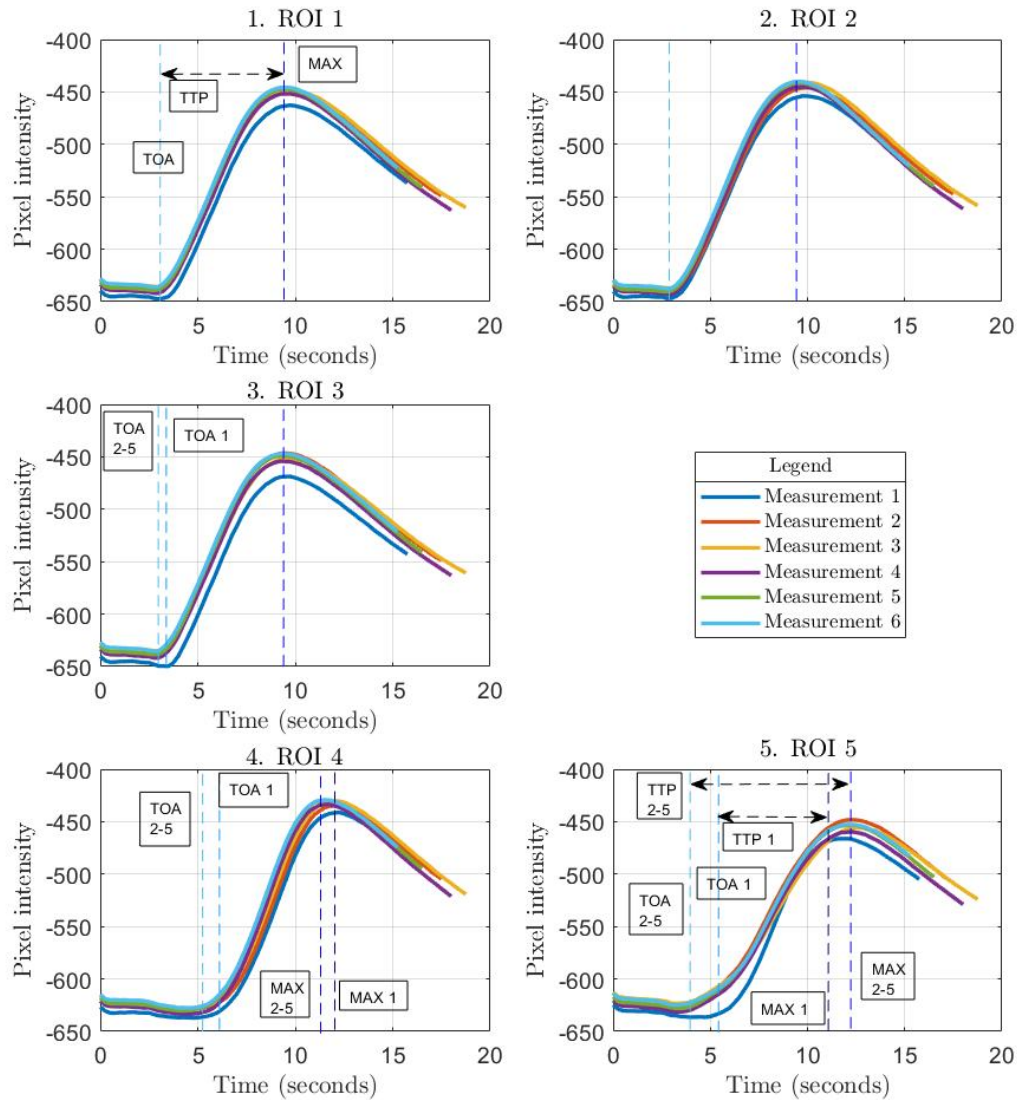


Fig. 5.5 Studying the reproducibility of the phantom set-up: time-intensity curves (TICs) of six measurements per region of interest (ROI)

Showing the time of arrival (TOA) and the time of the maximum value (MAX) of the curves. The TTP is shown as the difference between MAX and TOA.

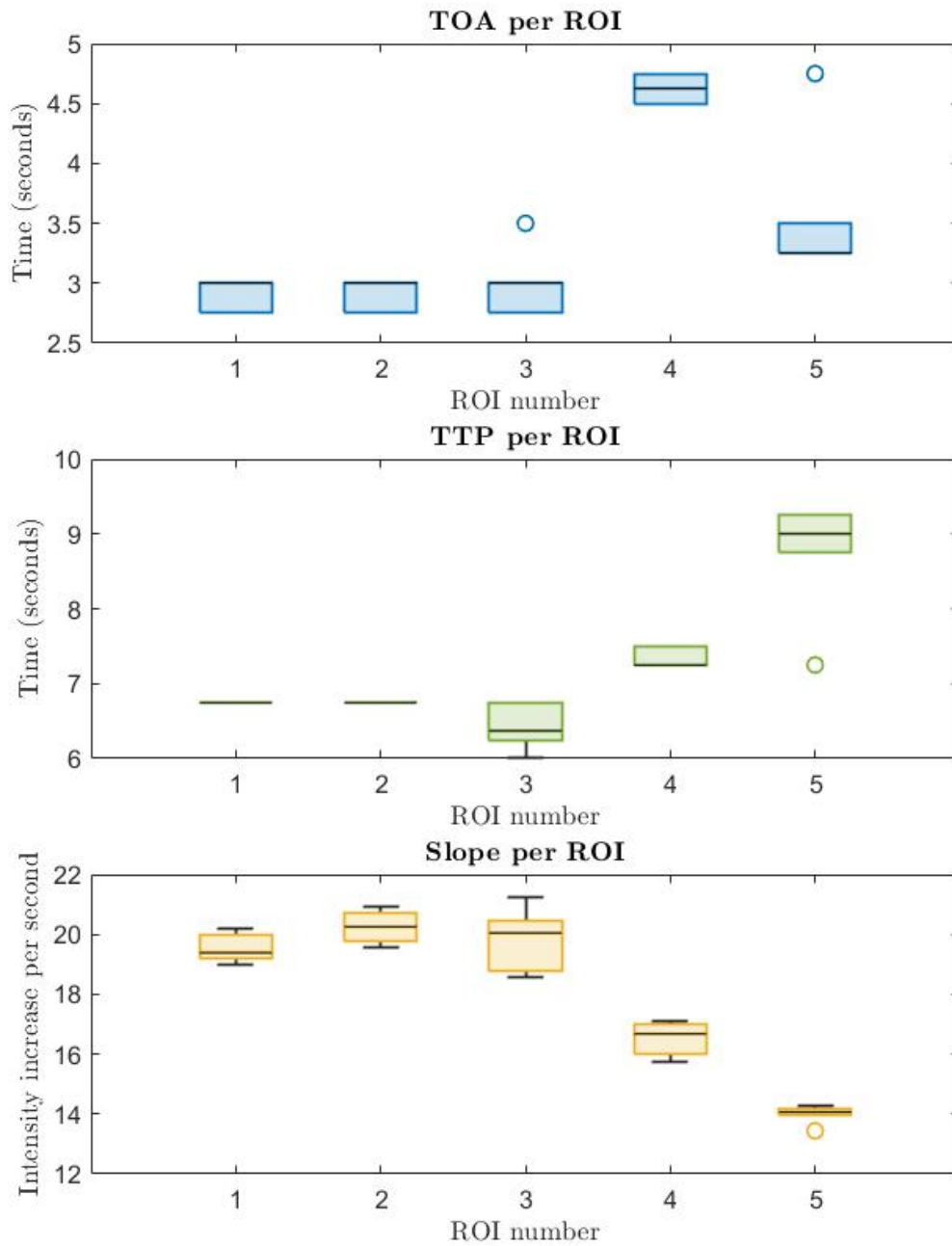


Fig. 5.6 Studying the reproducibility of the phantom set-up: Box-plots of the time-intensity curve values of six measurements (time of arrival (TOA), time to peak (TTP) and slope) per ROI

Both ROI 3 and ROI 5 have an outlier in the TOA measurements, in ROI 3 the standard deviations (std) are 9.13 % (TOA), 4.72% (TTP) and 5.13% (slope). In ROI 5 the std's are 16.95% (TOA), 8.67 % (TTP) and 2.11 % (slope).

The std's in ROI 1, ROI 2 and ROI 4 are < 4.4 % (TOA), < 1.7 % (TTP) and < 3.3 % (slope).

5.4 Effect of perfusion defect

Goal The aim of this experiment was to simulate a perfusion defect with the phantom and investigate the effect on the TICs.

Method Resistance tabs were added behind each compartment and the effect on the TICs of a partly (50%) closed tap and a fully closed tap (100%) behind one of the compartments was tested.

Hypothesis We expect to see a decreasing flow through the closed off compartment and hence a decreasing maximum contrast value and an increasing TTP.

Results Figure 5.7 shows the results. When the resistance behind the left compartment is increased the flow through the left compartment decreases and the flow through the right compartment increases.

Discussion and conclusion The results are in line with the expectations: the maximum contrast value decreases and the TTP increases due to the lower flow in the partly closed off compartment. This is what one would expect to see in patients with a perfusion defect as well. In these experiments, the effect of collaterals in the pathological situation was not taken into account. Collaterals will in some cases arise in patients with a perfusion defect, these bloodvessels influence the vascularisation structure to the affected tissue. The affected tissue will be partly perfused by the formation of the new vessels. In the TICs this will be visible as a higher intensity and longer time to peak, compared to the case of a perfusion defect without collaterals, as there is extra blood supply via a longer path. This can be simulated by placing a partition wall with holes between the compartments, instead of a solid partition wall (this idea was already described in section but should still be tested).

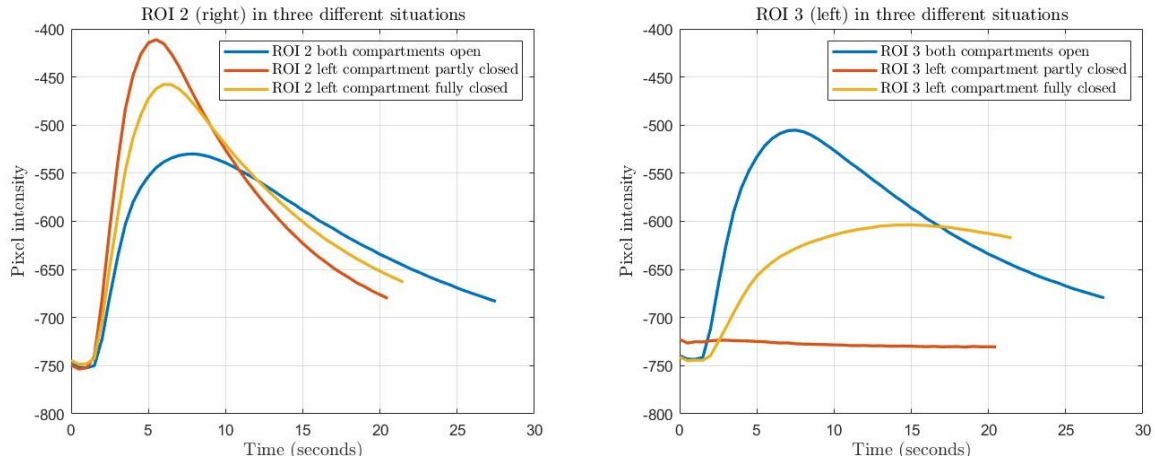


Fig. 5.7 Studying the effect of the simulated perfusion defect on the time-intensity curves (TICs) of the phantom. Three situations are shown, the resistance tab behind the left compartment fully open, partly closed and fully closed. When the left compartment is closed off, the left compartment (ROI 3) will have a lower flow and the right compartment (ROI 2) will have a higher flow (the maximum value increases and time to peak decreases).

5.5 Effect of flow velocity

Goal The aim of these experiments was to investigate the flow-velocity range of the phantom set-up and the effect of the flow-velocity on the TICs.

Method First, the lowest flow possible is applied, then, two steps are taken to the highest flow possible. This

results in four measurements with different flow-velocities. The set-up as described in section 6.3 is used.

Hypothesis We expect that when the flow is too low, the contrast will sink and not flush through the microcirculation compartment. Once the flow is high enough, a higher flow will lead to a lower TOA, TTM (time between the start of the measurement until maximum intensity) and TTP (TTM-TOA).

Results The results are shown in figure 5.8. In figure 5.8a the TICs of ROI 5 for different flow velocities is shown. When the flow increases the curves become smaller and the TOA, TTM and TTP decrease, as can be seen in figure 5.8b.

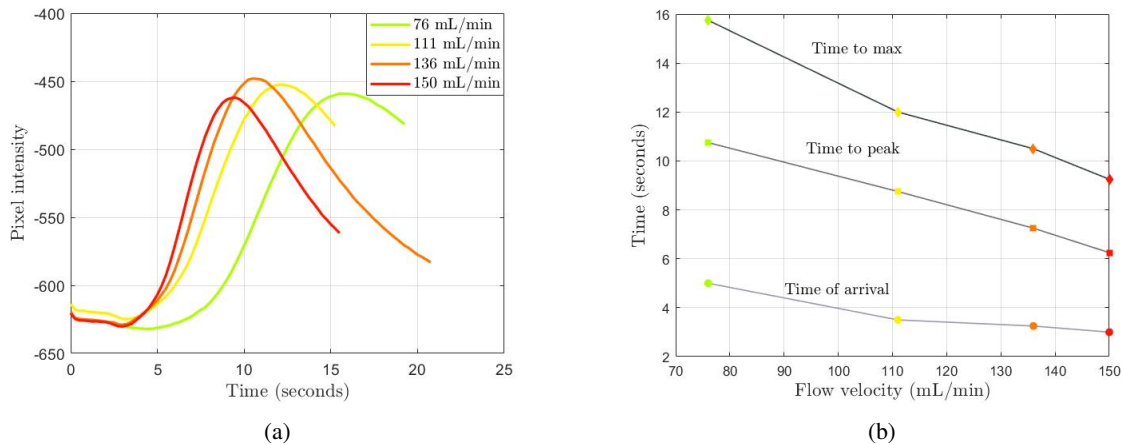


Fig. 5.8 Studying the effect of different flow velocities on the time-intensity curves (TICs) of the phantom: TICs (a) and values (b) of region of interest 5 for different flow velocities

Discussion When increasing the flow velocity, the time values decrease linearly. The lowest flow possible was 76 mL/min (through one compartment, so 150 in total), the resistance of the set-up was too high to generate a lower flow with the pump that we used. This is not in line with the tests done in section 4.2.2, where a flow of 104 mL/min in total was achieved. The difference can be explained by the fact that the set-up was adjusted before these experiments were carried out (section 6.3) and the resistance of the set-up was increased, making a lower flow impossible. With the minimum flow in this experiment, the contrast still flows through the phantom. To investigate what the minimum flow is for the contrast to flow through the phantom one could decrease the flow by letting part of the water output leak out before entering the phantom, by adding a tap in between the pump and phantom. The maximum flow possible was 150 mL/min through one compartment (300 mL/min through both compartments). A higher flow causes leaks, because the resistance in the set-up gets too high.

Conclusion The possible flow velocity ranges from 150 mL/min - 300 mL/min (input flow) and 75 mL/min - 150 mL/min through one compartment. When the flow increases the TOA, TTP and TTM decrease.

5.6 Effect of imaging system

Goal The aim of this experiment was to investigate the effect of different imaging systems on the TICs of the phantom.

Method The phantom is imaged with system 1 and 2, the flow-velocity and set-up are kept the same, and the TICs are compared.

Hypothesis We expect to see similar TICs.

Results In figure 5.9 the TICs of three measurement of ROI 1, computed with different imaging systems are shown. Table 5.1 contains the details of the measurements of the different scanners. The position of the phantom with respect to the source and the distance from source to detector was comparable in both systems. The main difference between the two scanners is the pixel intensity, which has a minimum value more than twice as low and a difference between minimum and maximum almost twice as high in the measurements obtained with system 1 compared to system 2. Another difference between the curves is how ‘smooth’ they are, the TIC of system 2 is smoother than the curve of system 1. The dip, present at about 2.5 seconds in the TIC of system 1, because of the arrival of contrast and scaling of the system (further explained in paragraph 5.8) does not seem to be present in system 2. The measurements with system 2 started later after the contrast bolus then the measurements in system 1, therefore the TOA and TTM in system 1 are later. The TTP is comparable.

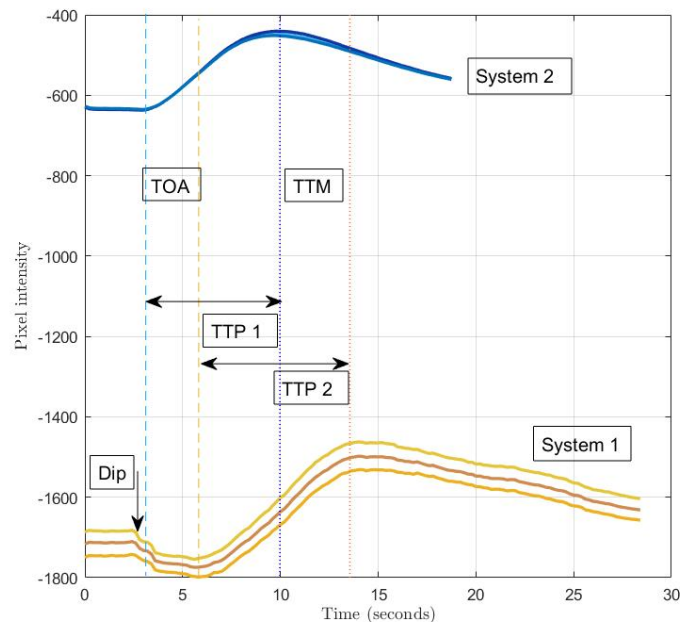


Fig. 5.9 Studying the effect of different imaging systems on the time-intensity curves (TICs) of the phantom: TICs of ROI 1 of two different imaging systems

Showing the time of arrival (TOA), time to max (TTM) and time to peak (TTP) for two series of 3 measurements at two different imaging systems. The dip in the TICs of system 1 is shown with a black arrow.

Discussion The difference in pixel intensity can be explained by the fact that the tube current in the measurements with system 1 was 1.7 times as high as the tube current in system 2. The higher the tube current, the higher the stream of electrons between the cathode and anode in the X-ray tube, resulting in a higher intensity of the X-ray output and a higher pixel intensity (lower in our graphs, because of the inversion). The tube current is chosen by the system itself, based on its own preferences and is not changeable. The smoothness of the curve depends on the amount of filtering that takes place. The post-processing in the two systems is different and unfortunately not open to those who are curious to see what happened behind the images.

Conclusion The TICs of the phantom obtained with different imaging systems have different intensity values due to different imaging settings (tube current and voltage) and post-processing procedures.

Table 5.1 Measurement specifications of angiography measurements with two different scanners

Measurement Imaging System	Contrast protocol Iodixanol 320 mg I/mL	Imaging protocol Frames per second	Imaging protocol kV	Imaging protocol mA	Distance source detector	Distance source patient
System 2	10 mL, 5 mL/s	FOOT 4	66	71	1031	820
System 1	10 mL, 5 mL/s	FL+ angio favor 2	55.5	119	1109	795

5.7 Effect of imaging protocol (framerate)

Goal The aim of this experiment was to test the effect of different clinical and experimental imaging protocols (the amount of frames per second) on the TICs.

Method Three different imaging protocols are used with different amounts of frames per second (fps). A higher fps will give a higher X-ray dosage.

1. 60s 2fps, 30s 1fps. A research protocol for measurements on the foot.
2. 90s 4fps. A protocol with a higher X-ray dosage.
3. 10s 2fps, 10s 1fps, 30s 0.5fps. The clinical protocol used during revascularisation procedures.

The measurements were stopped when the contrast was visually washed out of the phantom.

Hypothesis We expect to see a smoother curve with protocol 2 and similar curves with protocol 1 and 3.

Results In figure 5.11 the measurements with different protocols are shown. All measurements have the same shape, figure 5.10b shows the TICs zoomed into the top of the curve. Measurement 2 has a smoother curve, measurement 1 and 2 look the same.

Discussion The similarity around the peak of the curve of protocol 1 and 3 can be explained by the fact that the imaging protocol is the same during the first 10 seconds. Measurement two has a smoother curve because of the higher temporal resolution.

Conclusion The higher the temporal resolution the smoother the TIC.

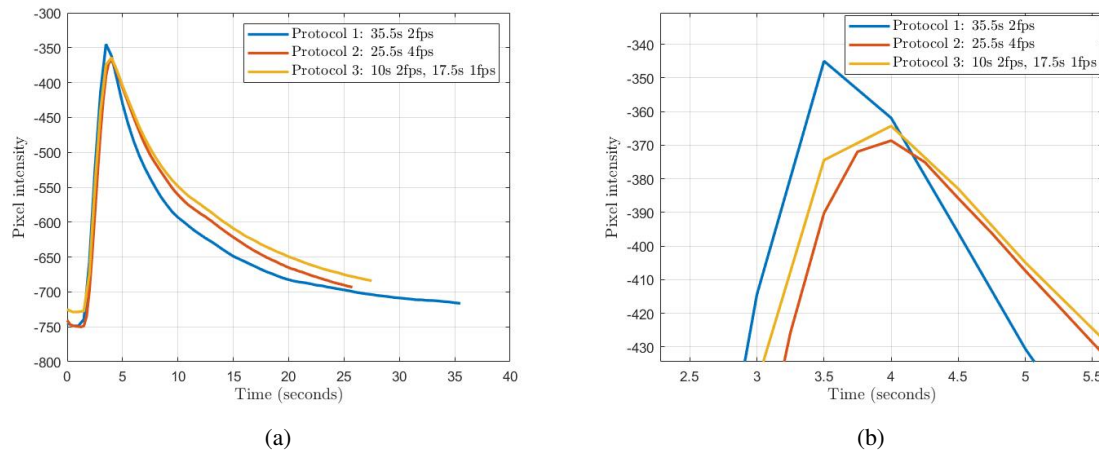


Fig. 5.10 Studying the effect of different imaging protocols on the time-intensity curves (TICs) of the phantom: TICs of ROI 1 with three different protocols, (a) the whole graph, (b) zoomed in on the peak
Protocol 1: blue, Protocol 2: red, Protocol 3: yellow

5.8 Scaling of the system

Goal The aim of these experiments was to test the behavior of the angiography imaging system: are there intensity changes over time due to the effects of automatic adjustments of the imaging system? And where do these adjustments come from?

Method This is investigated by adding a still standing contrast container as a reference next to the phantom in the field of view. During analyses a ROI was drawn on the contrast container (figure 5.11b) and the intensity over time was computed. If there are changes in intensity visible, it is explored where the possible changes are coming from: the modulation (changes in mA and kV values during measurement) will be turned off. The set-up as described in section 6.3 is used.

Hypothesis We would expect that the intensity of the contrast container would stay the same over time, as the contrast in the container is stagnant.

Results Figure 5.11a shows the TICs of all ROIs in two situations: when the dose reduction scheme of the system is turned on and off. When the dose reduction is turned on, the intensity of the contrast container drops once the contrast enters the microcirculation compartment of the phantom. The TICs of ROI 1-5 are smoother when the dose reduction is turned on. When the dose reduction is turned off the maximum intensity of ROI 1-5, and maximum intensity difference, are higher. When the dose reduction is turned off the TIC of the contrast container stays around zero.

Discussion The dose reduction schemes of the imaging system scale the mA and kV values during the measurement, when there is more contrast visible the amount of X-ray dosage is reduced, which results in a lower intensity difference between the first frame without contrast and the frame with maximal contrast; thus a lower maximum intensity and slope value.

It was investigated if the difference between the intensity difference (peak value minus baseline value) of the ROIs between scaling on and off was the same as the difference of the contrast container when the modulation was on. This was not the case. For example, ROI 5: when the modulation was on the base intensity was -1780, and the peak intensity -1110, the difference was 670. When the modulation was off the base intensity was

-1833, and the peak intensity -1489, the difference was 344. The difference between modulation on and off was 670-344 is 326. The difference of the peak intensity and baseline of the contrast container was 226. This means that using the contrast container to correct for the scaling is not directly possible.

In our latest set-up (as described in 6.3) the contrast agent first flows through a line alongside the phantom, and in the field of view, after which it enters the phantom. The dip and hill in figure 5.11a.1 and 5.11a.2 at three seconds can be explained by the contrast entering these lines (and thus the field of view), it would be expected that the scaling would happen at this moment as well, but that does not seem to be the case (as the contrast container intensity stays the same). However, the intensity values of the other ROIs do change at this moment. This could have something to do with the post processing of the imaging system: adjustments made at the back of the imaging system which we cannot see and are out of our control. These adjustments include more extreme windowing and levelling, which result in adjustments of the intensity/grey values.

These differences show that scaling happens in imaging systems and that it is hard to predict when it will happen and what causes it. In the case of TIC values, the time variables are not affected by scaling, but the intensity values are. When one wants to look at intensity values it is recommended to add a reference point to the phantom (like the contrast container) to see what happens with the intensity over time and further explore the possibility of correcting for the scaling.

Conclusion There are intensity value changes over time due to effects of adjustments of the imaging system. These adjustments are initiated by dose reduction schemes and post processing processes of the imaging system.

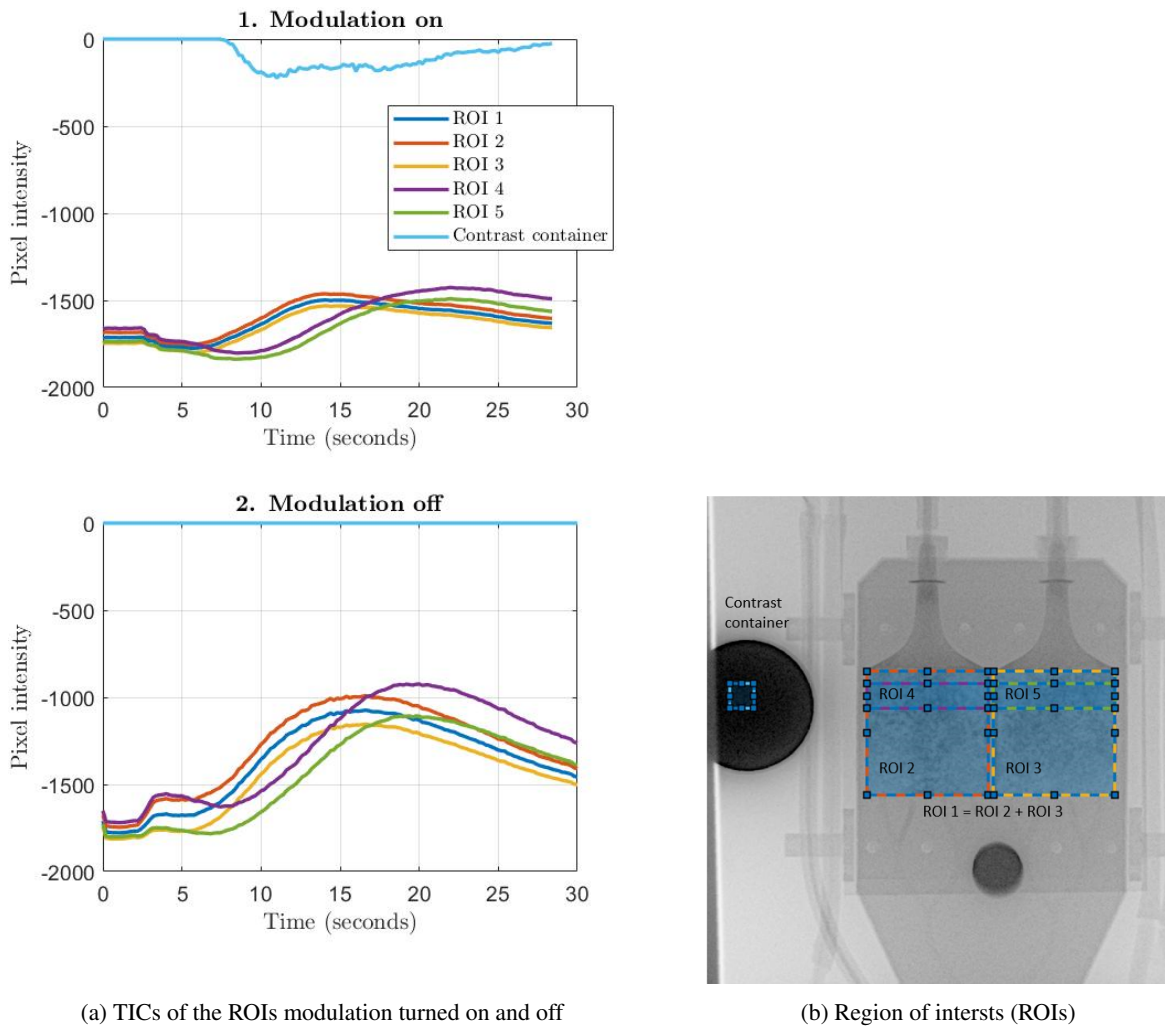


Fig. 5.11 Studying the effect on the time-intensity curves (TICs) of turning the modulation of the imaging system on and off

(a) Shows the TICs of the ROIs when the modulation is turned on and off, the modulation is clearly visible in the TIC of the ROI of the still standing contrast container, as the intensity changes during the measurement. (b) shows the ROIs of the phantom

5.9 Conclusions of 2-D phantom perfusion measurements

The phantom set-up was tested and 2-dimensional phantom perfusion imaging with C-arm CT was studied. With the phantom, realistically shaped TICs and reproducible time variables were acquired. The phantom can simulate a perfusion defect and the flow velocity can be controlled, both features affect the TICs in the way that is also expected to be seen in patients with reduced perfusion in the lower extremities. It was learned that the intensity variables are highly dependent on the choices made by the imaging system; these include the choice of tube current and tube voltage during the scout scan, modulation of these values during measurement (dose reduction schemes), and post-processing protocols after the measurement. These options differ between imaging systems and are out of our control. Based on these findings we would recommend further investigation

of perfusion quantification (in the lower extremities), based on the time variables of the TICs, since drawing conclusions from the intensity variables is complicated due to all the variability described above. All in all, the phantom set-up performed according to our expectations, the next step would be to validate the set-up with more measurements and test it with 3-dimensional imaging modalities (first CT perfusion and then cone-beam CT).

6 | Testing the phantom: studying 3 - dimensional phantom perfusion imaging with CT

The aim of the CT perfusion experiments at UMCG was to perform another proof of concept test: would it be possible to obtain a realistically shaped time-intensity curve (TIC) with the phantom, when using a CT perfusion imaging system and the brain perfusion imaging protocol and clinical software?

6.1 Analyses method: application of clinical software in CT perfusion measurement

The CT perfusion measurements are performed at UMCG. The CT systems are Siemens SOMATOM Force and FLASH CT systems, both offering the ability to complete brain perfusion imaging protocols. The clinical software used to analyse the perfusion CT images is Syngo.via. With the software, we aim to make TICs of the phantom and acquire the TIC values. The workflow of the analyses is summarized in appendix D.

6.2 First measurements and corrections to be made

Goal In this first experiment the aim was to obtain a realistically shaped TIC with the phantom, when using a CT perfusion imaging system and the brain perfusion imaging protocol.

Method The phantom set-up was build up on the CT scan table. The lowest pump setting was used, which resulted in a flow of of 65-85 mL/min per flow sensor, so a total inflow of 130-170 mL/min. A contrast protocol of 10 mL in 5mL/sec was used. The brain perfusion scanning protocol was selected, and after the measurements the CT scans were loaded into the clinical software 'Syngo.Via,' to perform the analyses and obtain TICs.

Results It was not possible to compute TICs of the phantom with the clinical software.

Discussion The clinical software could not compute TICs due to (at least) two problems. Firstly, the field of view of the CT brain perfusion scan is only 11cm, therefore the arterial input and venous outflow could not be imaged simultaneously. However, the software needs to have an arterial input and venous outflow in order to make the TICs. The other problem encountered was during the vessel definition step, due to the absance of difference in contrast intensity between the AIF and tissue. The clinical software defines vessels based on the HU value of the AIF, which is used as a baseline, the HU value of 'tissue' should be lower then the baseline value to be recognized as tissue. Figure 6.1 shows an image of the segmentation of the arterial input made by

the program: because the contrast intensity in the microcirculation compartment is the same as in the incoming vessels, the microcirculation is segmented as incoming artery as well. From these experiments we learned that two adjustments need to happen: having the arterial input and venous outflow in the field of view and creating a difference in contrast intensity between the AIF and microcirculation compartment.

Conclusion With the current phantom set-up TICs cannot be obtained when using a CT perfusion imaging system and the brain perfusion imaging protocol, therefore, the phantom set-up needs to be adjusted.

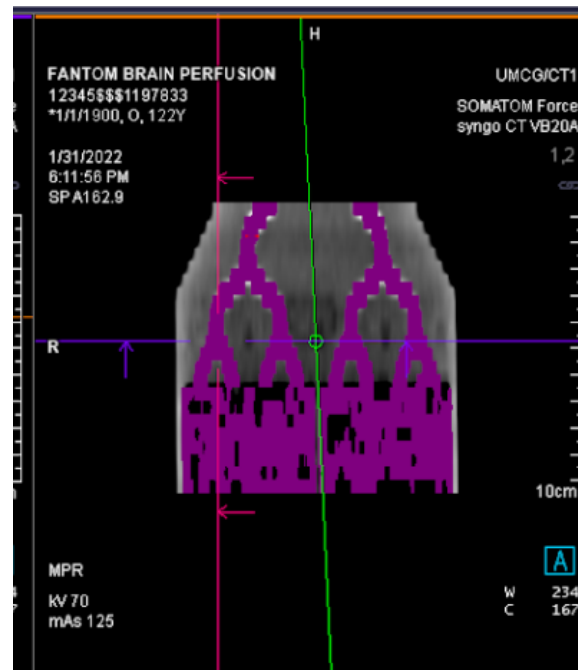


Fig. 6.1 CT perfusion measurement of the phantom analysed with Syngo.via clinical software
The clinical software segments the microcirculation compartment as incoming vessel (purple colour)

6.3 Re-design: phantom enhancements for recognition by the clinical software

The design of the phantom is adjusted based on two new requirements:

- The arterial input and venous outflow need to be in the field of view (11 cm length x 70 cm width)
- The contrast intensity should be lower in the microcirculation compartment than in the arterial input

The adjustments made are schematically shown in figure 6.2. The arterial input and venous outflow are in the field of view and a bypass will reduce the contrast inflow into the microcirculation compartments. With these adjustments CT perfusion image analyses with the clinical software should be possible.

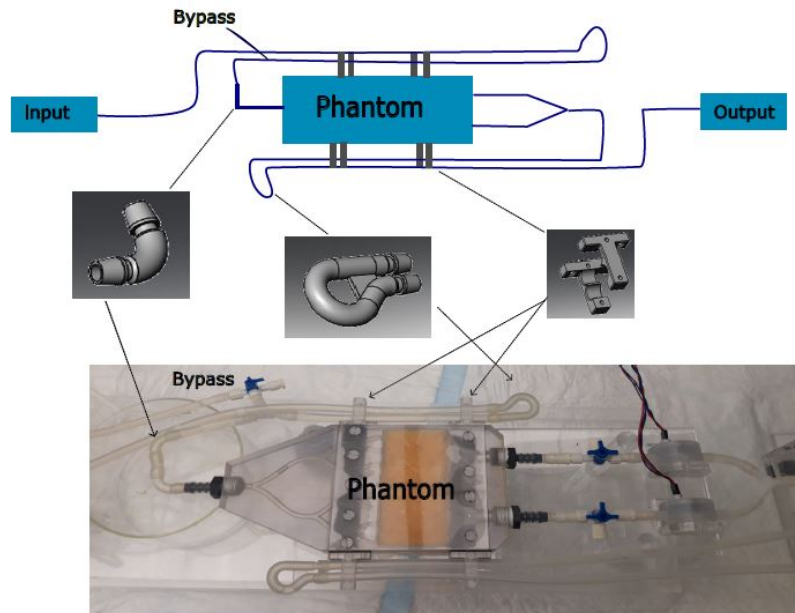


Fig. 6.2 The adjusted phantom set-up

The upper image schematically shows the adjustments: the ingoing and outgoing tubes run alongside the phantom and are connected to the phantom via three different connection pieces. A bypass lets part of the ingoing fluid out before entering the phantom. The result is shown in the lower picture.

6.4 Second set of experiments and conclusions

Goal The aim of the second set of experiments was to investigate whether realistically shaped TICs could be obtained with the adjusted phantom set-up, using a CT perfusion imaging system and the brain perfusion imaging protocol. Sub-questions include:

- What is the effect of the added tubes (having the arterial input function (AIF) in the field of view) on the analyses?
- What is the effect of opening the bypass?
- What is the effect of contrast dilution on the AIF and segmentation?
- How do the TICs and AIF compare with the TICs and AIF of the brain?

Method Five experiments were performed, the specifications of each experiment are summarised in table 6.1. The CT perfusion scans are analyzed using Syngo.via (see section 6.1), the ROIs are chosen manually at the same location and with the same size in each measurement.

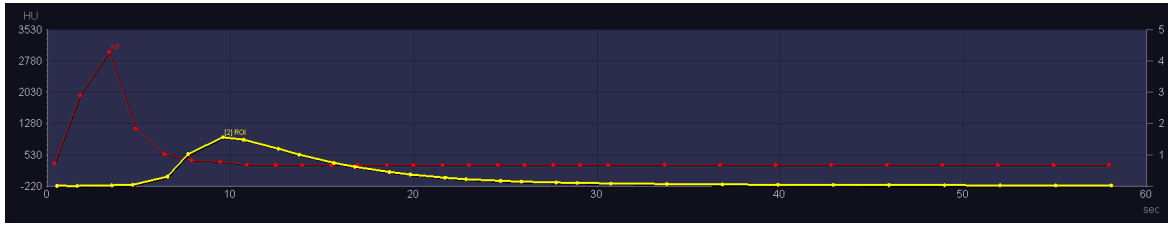
Table 6.1 Protocols of the second set of perfusion CT experiments

Experiment	Flow rate (mL/min)	Contrast protocol	Imaging protocol	Bypass tab
1.	100 mL/min per flow sensor (200 mL/min in total)	5 mL in 2.5 mL/sec	Brain perfusion	Closed
2.	60 mL/min per flow sensor (120 mL/min in total)	5 mL in 2.5 mL/sec	Brain perfusion	75% open
3.	35 mL/min per flow sensor (70 mL/min in total)	5 mL 70% mixed with water in 2.5 mL/sec	Brain perfusion	100% open
4.	85 mL/min per flow sensor (170 mL/min in total)	5 mL 70% mixed with water in 2.5 mL/sec	Brain perfusion	50% open
5.	100 mL/min per flow sensor (200 mL/min in total)	5 mL 70% mixed with water in 2.5 mL/sec	Brain perfusion	Closed

Results The TICs of the different measurements are shown in figure 6.3 . Table 6.3 contains the CBF, CBV, TTM, TTP, and MTT of all measurements. In table 6.2 it can be seen that the CBF and CBV increase and decrease together, confirming the central volume principle [64]. The flow was related proportionally to the CBF and CBV, and inversely to the time parameters. As seen in experiment 3, the flow through the phantom is lower when the bypass tab is opened more, causing the contrast to sink in the sponge and maxing out the HU values, hence maxing out the CBF and CBV. Experiment number 4 yielded the best results in the vessel definition step without sinking of the contrast agent in the sponge, with a flow of 85 mL/min, the bypass 50% opened, and the contrast diluted 70% with water. Taking the contrast line as AIF did not make a difference compared to taking the incoming tube as AIF. The effect of contrast dilution is a slightly lower maximum HU value in the AIF (measurement 1 vs measurement 5 in figure 6.3). Figure 6.4 shows the TIC of measurement 4 and the TIC of a patient measurement of the brain. In the patient measurement, the HU values are lower and therefore CBF and CBV are also lower (50 times).

Table 6.2 Cerebral blood flow (CBF) calculated based on flow sensors and clinical software and the Cerebral blood volume (CBV) calculated by the clinical software

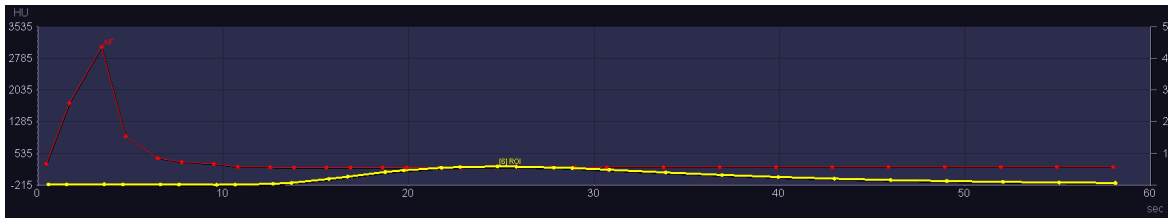
	Flow (flow sensors) (mL/min)	CBF (based on flow sensor) (mL/min/100 mL)	CBF (Syngo.via) (mL/min/100mL)	CBV (Syngo.via) (mL/100mL)
1.	100	330	1239	185
2.	60	200	2500	292
3.	35	117	3071	307
4.	85	283	1400	169



(a) Measurement 1, closed bypass, contrast not diluted



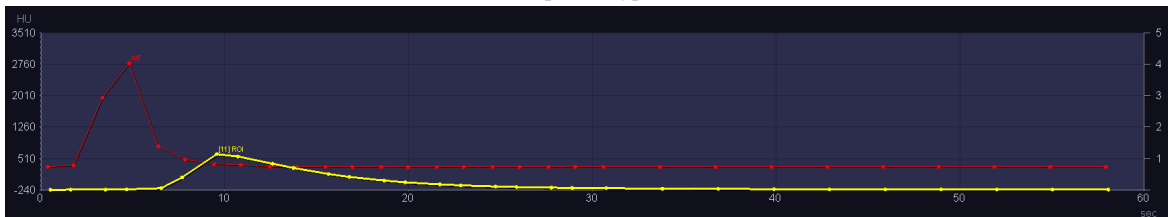
(b) Measurement 2, 75% opened bypass, contrast not diluted



(c) Measurement 3. 100% opened bypass, 70% diluted contrast



(d) Measurement 4, 50% opened bypass, 70% diluted contrast



(e) Measurement 5, closed bypass, 70% diluted contrast

Fig. 6.3 Time-intensity curves in Syngo.via for five different measurements

Table 6.3 Results of the second set of perfusion CT experiments

Experiment	Flow rate (mL/min)	CBF (mL/min/100mL)	CBV (mL/100mL)	TTM (sec)	TTP (sec)	MTT (sec)
1. Closed bypass, normal contrast	100	1239	185	8.5	9.58	9
2. 75% open bypass, normal contrast	60	2500	292	9.92	12.45	9.58
3. 100% open bypass, 70% diluted contrast	35	MAX	MAX	23.76	24	19
4. 50% open bypass, 70% diluted contrast	85	1400	169	7	9.49	7.43
5. Closed bypass, 70% diluted contrast	100	MAX	MAX	7.35	9.57	7.55

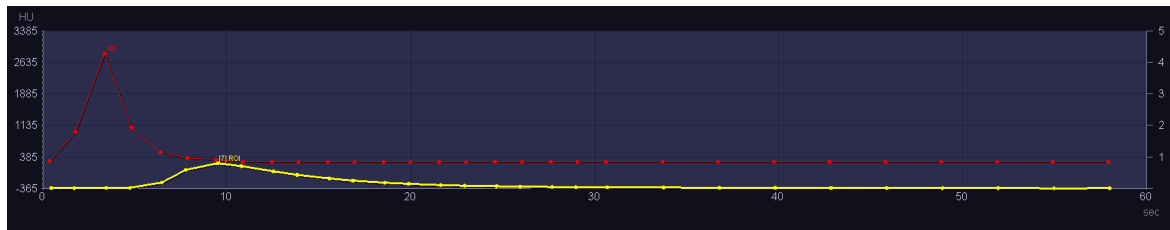
Discussion and conclusion With the phantom set-up, TICs of the CT perfusion measurements in the clinical software can be obtained. However, the shape and values of the TICs do not resemble the values of human data. Adjustments to the phantom set-up need to be made to mimic the human physiology and TIC values as much as possible. Recommendations of adjustments and the reasoning behind them are described in this section.

Reference vessel and venous outflow

In the adjusted phantom set-up design, the venous outflow was positioned in the field of view, because of the assumption that the clinical software needed to have both the arterial input as well as the venous outflow. This assumption was wrong. The program required an arterial input and reference vessel, which did not necessarily had to be the venous outflow. In figure 6.4 the TICs of the phantom (AIF and ROI), ROIs of a patient, and, the AIF and reference vessel of a patient are shown. The patient measurement contains both a TIC of the AIF and a reference vessel (6.4c). The reference vessel is used as a reference point for the calculation to define the maximum enhancement value. The clinical software uses this value to define the windowing percentage and cut-off values for vessel definition. It is however not necessary to have both an AIF and reference vessel when the vessel picked is large enough to serve as both (the AIF will serve as a reference vessel, and there will only occur a TIC of the AIF). Unfortunately, there is no clear answer to how large the vessel's diameter should be, this is something that should be investigated during the next phase of the phantom's development.

Arterial input function

The AIF of the phantom (figure 6.4a) is ten times too high and the shape of the graph is incorrect, compared to patient measurements (figure 6.4c). The AIF in the patient measurement rises and descends more slowly, and has a lower HU value. In the case of patients, a contrast bolus is injected, which results in laminar flow through the arteries towards the artery of interest. This laminar flow causes a certain delay and dispersion in the circulatory system, which influences the results of the AIF. The delay leads to a temporal shift of an AIF and dispersion causes a change in the shape of the curve. [65, 66] Bredno et al., created a brain perfusion simulation model to simulate realistic patient data.[65] The model presents AIFs and TICs for several flows and



(a) Measurement 4 of the phantom



(b) Patient Measurement ROIs



(c) Patient Measurement ROI, AIF and reference vessel

Fig. 6.4 Time-intensity curves in Syngo.via for CT perfusion measurements of the phantom (a), TICs of the ROIs of a patient (b) TICs of ROI, AIF and reference vessel of a patient (c)

perfusion states. Theoretical models like these could be used to get to a correct AIF with the phantom set-up. We recommend mimicking the AIF of patients by adjusting the bolus injection technique, with the help of a multi-phase dual injection pump, to pump water (for dilution) and contrast with different injection phases and simulate the delay and dispersion that happens in patients.

HU values

As a result of the incorrect arterial input and due to the high amount of contrast relative to the sponge, the maximum HU values in the ROIs of the microcirculation compartment are also 5-10 times as high compared to human values. The CBV and CBF get high and in some measurements max out, presumably due to pooling of the contrast. The minimum HU values are between -364 and -230, whereas the values of the brain are just above zero (between 30 and 40 HU (figure 6.4b)). The HU value of water is zero and the HU value of air is -1000. The sponge material presumably has too much air in it even though it is thoroughly flushed with water and checked for air bubbles. Another reason for the low HU values could be the way that the clinical software adjusts the measurements. To find out if the HU of the material is that low or higher, we recommend looking at the raw data of the CT scan to find out what the real HU of the material is. If the high HU value results from (micro) air bubbles in the sponge we recommend looking at another material.

Analysis

The material of the sponge has a characteristic perfusion pattern. This can be seen as an advantage because of the distinctive perfusion structure which does not change over the measurements, however, with a more homogeneous flow the TIC values are more controllable throughout the microcirculation compartment when the pumping output is changed.

Another point of interest in CT brain perfusion measurements with the phantom set-up is the analysis method. ROI selection in Syngo.via is manual as the phantom is not recognized as a brain, therefore, small changes in the positioning of the ROI can lead to different results across measurements. We repeated the analysis steps on the same measurement multiple times and got the same results, so the analysis is reproducible when used in the same software on the same measurement. However, we did not perform experiments with the same settings twice with some time in between to investigate the differences in the analysis. In the next phantom design, markers could be incorporated that light up on the CT scan and make manual ROI selection more standardized. Another possibility is to adjust the phantom set-up so that the clinical software recognizes the phantom as a brain and automatically segments it in that way. This can be tested by adding a circular object around the phantom and analyzing the images in Syngo.via. When this is not possible and the phantom is used for comparison, the small changes in ROI selection should be dealt with.

New requirements

When choosing another material for the microcirculation compartment this material should meet the following new requirements to get closer to physiological values:

- The HU value of the material when saturated with water should be around zero.
- The flow through the microcirculation material should be between 10 mL/100 gr/ min (CBF ischaemic core of stroke patients) and 60 mL/100 gr/ min (CBF healthy brain tissue).[66, 67] The correct balance needs to be found between the choice of material, the opening of the bypass, and contrast dilution without stagnation of the contrast in the material and achieving a normal HU density.

We recommend looking into membranes, such as dialysis tubing (cellulose acetate) as the next microcirculation compartment material. Care must be taken of how to align the fine tubes in the compartment and avoid them from getting out (use a filter at the beginning and end of the microcirculation compartment).

Validation of acquired values

To investigate whether the acquired values of the phantom for the CBV, CBF, and MTT with Syngo.via are correct, they should be related to the actual flow in the microcirculation compartment. At the moment, the CBF and CBV given by Syngo.via are very high, most likely as a result of the HU values which are incorrect. In the first attempt of determining the actual flow in the microcirculation compartment, the flow in the flow sensors is directly related to the flow in the microcirculation compartment. The volume in the microcirculation compartment is 30,0 mL (without sponge) and the flow measured in the flow sensors is mL/min, the CBF is in mL/100gr/min (= mL/100mL/min because of the density of water). A flow of 100 mL/min measured with the flow sensors in 30 mL, would give a CBF of 330 mL/min/100mL. Following these steps the CBF based on the flow sensors is given in table 6.2, next to the CBF calculated by Syngo.Via.

Figure 6.5 shows the relationship between the reference flow ($Q_{phantom}$) and the measured flow with the clinical software. The high correlation ($\rho=-0.98$) is physiologically incorrect and the dataset is too small to draw any conclusions, but it does show the potential of the phantom set-up. It should be further investigated how Syngo.via calculates the CBF and CBV and how this can be related to the CBF and CBV calculated based on the information from the flow sensors. Future research should aim at completing the validation step in order to make the phantom useful for quantification.

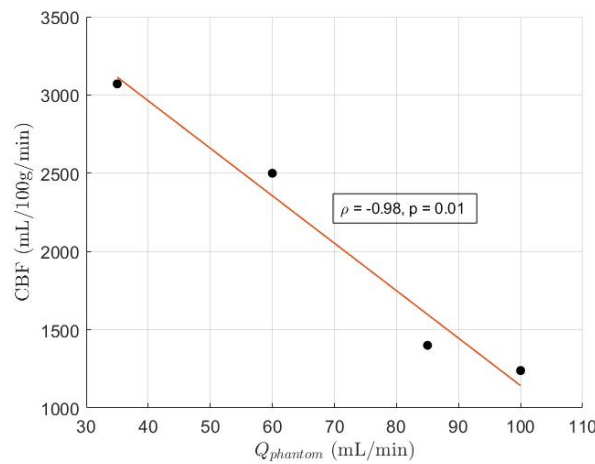


Fig. 6.5 Correlation plot of the reference flow ($Q_{phantom}$) and measured flow (CBF) with the clinical software. ρ is the Pearson correlation coefficient.

7 | Discussion and conclusion

The aim of this research project was to develop a perfusion phantom set-up of the vascularisation of the lower extremities and study quantitative perfusion imaging with 2-D perfusion angiography. Furthermore, the secondary goal was to study quantitative perfusion imaging of the vascularisation of the brain with CT perfusion by making small adjustments to the phantom set-up. The study objectives included:

1. Determining the program of requirements for the phantom set-up
2. Translating the program of requirements to a design of the phantom set-up
3. Testing and evaluating the phantom set-up on the program of requirements

After performing a market research, where the clinical demand for a perfusion phantom was explored and knowledge was gained from commercially available phantoms and state-of-the art research, the program of requirements for the phantom set-up was determined. The phantom set-up was tested and evaluated on the program of requirements for two clinical applications: imaging of the perfusion of the lower extremities with 2-D perfusion angiography and imaging of cerebral perfusion with CT perfusion.

7.1 Phantom design and realisation

With the phantom set-up TICs of the microvasculature perfusion can be made and a perfusion defect can be simulated. The set-up can give reproducible results and is applicable for angiography and CT perfusion. The phantom consists of a macrovasculature vessel structure which branches into the microcirculation compartment.

However, simplifications have been made during the translation process from phantom requirements to phantom design specifications. The diameters of the incoming arteries and branches are all 0.31 cm instead of 0.22 cm and decreasing over the branches, as the 3-D printed vessel structure, filled with support material, needed to be opened manually after printing. This process could get impossible when the diameter of the vessels is too small, based on the opening experience it is believed that the diameter could be 0.05 cm smaller than the current diameter. It is however the question if this is necessary for the application that the phantom is used for. If it is possible to get to an AIF and TICs similar to patient data with the current set-up it is not necessary to adjust the diameter.

The phantom cannot simulate the blood flow velocity in the same ranges as both the lower extremities as well as the brain. During the initial tests of the phantom set-up it was concluded that the output volume of the pump could not reach the lower boundary as drawn up in the requirements (100 mL/min, where 30 mL/min was required to simulate the incoming flow in the a. Tibialis posterior). With opening the bypass, which

was implemented for the CT perfusion measurements (section 6.3), the flow could be reduced. A flow of 30 mL/min will however let the contrast sink in the phantom, and if this flow velocity is necessary a different microcirculation material should be used. A lower incoming flow can be used to obtain a longer time to peak in the microcirculation compartment and make that more similar to human values.

7.2 Phantom testing and evaluation

7.2.1 Perfusion phantom application in 2-D perfusion imaging of the lower extremities with C-arm CT

We succeeded in developing a reproducible perfusion phantom set-up for 2-D perfusion imaging with C-arm CT. The flow velocity can be controlled and a perfusion defect can be simulated. The measurements can be analysed in a standardised way with the semi-automated analysing method for 2-D perfusion imaging measurements. The effect on the time-intensity curves (TICs) of different imaging systems and dose reduction schemes was studied. From the experiments it was learned that the intensity variables in the TICs are dependent on the choice of tube current and tube voltage during the scout scan, modulation of these values during measurement (dose reduction schemes), and post-processing protocols after the measurement. These findings are of importance in the research of quantitative perfusion analyses with C-arm CT, as they can cause inter-system, inter-patient, and inter-measurement variabilities. Based on the findings two recommendations are made: investigate the possibility of correction for dose reduction schemes and, further investigation of perfusion quantification (in the lower extremities) based on the time variables of the TICs instead of the intensity variables as these are not affected by the difference in imaging system and dose reduction schemes. In this way our phantom set-up could possibly help in the search for a reliable measure for microcirculation perfusion in the lower extremities, which could possibly improve disease management of patients with critical limb ischaemia.

7.2.2 Perfusion phantom application in 3-D perfusion imaging of the brain with CT perfusion

By adjusting the phantom set-up to have the arterial input in the field of view and a bypass tab to let out part of the contrast, TICs of the phantom with the clinical software of CT perfusion measurements were acquired. The time-intensity curves do however not resemble patient measurements yet, in the discussion of section 6.4 the current shortcomings of the set-up were evaluated and recommendations for future research were made.

It is suggested to start with finding a different material; This material should have a HU value of around zero when saturated with water and a flow of contrast agent of 60 mL/min/100gr should be possible without sinking of the contrast. Furthermore, the arterial input of the contrast bolus injection in a patient needs to be mimicked, by finding the right bolus injection technique with the help of a multiphase dual injection pump. Last of all, the analyzing method needs to be standardized, it should be investigated how the flow sensor data can be related to the CBF and CBV values of the clinical software and, it needs to be investigated if the phantom should look more like a human head. Boese et al [42], developed a CT perfusion phantom specifically for brain perfusion and studying C-arm perfusion imaging. The phantom was designed based on the anatomy of the human head, in this way the software did recognize the phantom as a brain and the correct dose was applied. Their research succeeded in making CT perfusion maps on both conventional CT and C-arm systems.

Once realistic TICs with the phantom can be realized with CT perfusion, it can be investigated if perfusion maps with the new cone-beam CT (CBCT) system at the UMCG can be acquired. In further steps, the CBCT perfusion maps need to be related to the phantom flow data to investigate if a reliable quantitative perfusion measure can be acquired with CBCT. With this research we hope to get one step closer to improving disease management of patients with acute stroke, by excluding the extra stop at the CT perfusion and including CBCT as the modality for diagnostics at the angiography suite, time can be saved.

7.3 Validation and application

The simplifications made in the phantom design are considered acceptable for this first stage of phantom development and the application that it is used for: studying the response of 2-D perfusion angiography and CT perfusion imaging. Nevertheless, without validation of the CT perfusion measures, quantitative CT perfusion imaging with the phantom will not give reliable results. Future research should aim at solving this validation step, to extend the application domain of the phantom set-up.

The phantom set-up has a straightforward and modular design, and could therefore be widely applicable. With minor changes, it can be used with multiple modalities and for different clinical applications. The set-up is for example already used to study perfusion imaging with fluorescence angiography for the clinical application of intestinal microcirculation, the 3-D printed microcirculation compartment was changed for a dialyzes cartridge and the flow set-up was used for the perfusion and application of fluorescence marker.

7.4 Conclusion

The ultimate goal of this research project was to facilitate ground-truth evaluation of image-derived tissue perfusion measures in the clinical setting. In this work we focussed on the development of a perfusion phantom set-up dedicated to angiographic imaging of the microcirculation in the lower extremities and CT perfusion imaging of the brain. All in all, a versatile perfusion phantom set-up applicable for 2-D perfusion imaging with C-arm CT is designed and realised. With small changes the set-up could be suitable for multi-modality and multi-disease purposes and may provide necessary insights in perfusion imaging techniques.

References

- [1] Blood vessels: Types, anatomy, function and conditions, <https://my.clevelandclinic.org/health/body/21640-blood-vessels>.
- [2] Cardiac output: Normal rate, low output causes and how to increase it, <https://www.webmd.com/heart/heart-cardiac-output>.
- [3] Hart- en vaatziekten in nederland 2019 cijfers over incidentie prevalentie ziekte en sterfte, <https://www.hartstichting.nl/getmedia/41cf66bf-2107-44d6-b2c3-739fc465ec73/cijferboek-hartstichting-hart-vaatziekten-nederland-2019-rp92.pdf>.
- [4] J Frostegård. Sle, atherosclerosis and cardiovascular disease. *Journal of internal medicine*, 257(6):485–495, 2005.
- [5] E Calzia, Z Iványi, and P Radermacher. Determinants of blood flow and organ perfusion. *Functional hemodynamic monitoring*, pages 19–32, 2005.
- [6] Jeffrey L Saver. Time is brain—quantified. *Stroke*, 37(1):263–266, 2006.
- [7] Harold P Adams Jr, Gregory Del Zoppo, Mark J Alberts, Deepak L Bhatt, Lawrence Brass, Anthony Furlan, Robert L Grubb, Randall T Higashida, Edward C Jauch, Chelsea Kidwell, et al. Guidelines for the early management of adults with ischemic stroke: a guideline from the american heart association/american stroke association stroke council, clinical cardiology council, cardiovascular radiology and intervention council, and the atherosclerotic peripheral vascular disease and quality of care outcomes in research interdisciplinary working groups: the american academy of neurology affirms the value of this guideline as an educational tool for neurologists. *Stroke*, 38(5):1655–1711, 2007.
- [8] Kai Niu, Pengfei Yang, Yijing Wu, Tobias Struffert, Arnd Doerfler, Sebastian Schafer, Kevin Royalty, Charles Strother, and G-H Chen. C-arm conebeam ct perfusion imaging in the angiographic suite: a comparison with multidetector ct perfusion imaging. *American Journal of Neuroradiology*, 37(7):1303–1309, 2016.
- [9] Steve Duff, Michael S Mafilios, Prajakta Bhounsule, and James T Hasegawa. The burden of critical limb ischemia: a review of recent literature. *Vascular Health and Risk Management*, 15:187, 2019.
- [10] Bryan Wermelink, Kirsten F Ma, Marieke Haalboom, Mostafa El Mounni, Jean-Paul PM De Vries, and Robert H Geelkerken. A systematic review and critical appraisal of peri-procedural tissue perfusion techniques and their clinical value in patients with peripheral arterial disease. *European Journal of Vascular and Endovascular Surgery*, 62(6):896–908, 2021.
- [11] Jim A. Reekers, Mark J. W. Koelemay, Henk A. Marquering, and Ed T. van Bavel. Functional imaging of the foot with perfusion angiography in critical limb ischemia. *Cardiovascular and Interventional Radiology*, 39:183, 2 2016.
- [12] Holger Lawall, Peter Huppert, Christine Espinola-Klein, and Gerhard Rümenapf. The diagnosis and treatment of peripheral arterial vascular disease. *Deutsches Ärzteblatt International*, 113:729, 10 2016.
- [13] Jun Shu and Gaetano Santulli. Update on peripheral artery disease: Epidemiology and evidence-based facts. *Atherosclerosis*, 275:379, 8 2018.

- [14] Iacopo Fabiani, Enrico Calogero, Nicola Riccardo Pugliese, Rossella Di Stefano, Irene Nicastro, Flavio Buttitta, Marco Nuti, Caterina Violo, Danilo Giannini, Alessandro Morgantini, Lorenzo Conte, Valentina Barletta, Raffaella Berchiolli, Daniele Adami, Mauro Ferrari, and Vitantonio Di Bello. Critical limb ischemia: A practical up-to-date review:. <https://doi.org/10.1177/0003319717739387>, 69:465–474, 11 2017.
- [15] Marie D Gerhard-Herman, Heather L Gornik, Coletta Barrett, Neal R Barshes, Matthew A Corriere, Douglas E Drachman, Lee A Fleisher, Francis Gerry R Fowkes, Naomi M Hamburg, Scott Kinlay, et al. 2016 aha/acc guideline on the management of patients with lower extremity peripheral artery disease: executive summary: a report of the american college of cardiology/american heart association task force on clinical practice guidelines. *Journal of the American College of Cardiology*, 69(11):1465–1508, 2017.
- [16] Richtlijn 'diagnostiek en behandeling van arterieel vaatlijden van de onderste extremiteit' van de nederlandse vereniging voor heelkunde | nederlands tijdschrift voor geneeskunde.
- [17] Peripheral arterial disease avis vascular centre, <https://www.avisvascularcentre.com/peripheral-arterial-disease-pad-is-treatment-required/>.
- [18] Beroerte, <https://www.hartstichting.nl/hart-en-vaatziekten/beroerte>.
- [19] Beroerte, <https://www.mmc.nl/neurologie/aandoeningen-en-behandelingen/beroerte>.
- [20] Anthony M Kaufmann, Andrew D Firlik, Melanie B Fukui, Lawrence R Wechsler, Charles A Jungries, and Howard Yonas. Ischemic core and penumbra in human stroke. *Stroke*, 30(1):93–99, 1999.
- [21] Stroke headway the brain injury association, <https://www.headway.org.uk/about-brain-injury/individuals/types-of-brain-injury/stroke/>.
- [22] Sjoerd Jens, Henk A Marquering, Mark JW Koelemay, and Jim A Reekers. Perfusion angiography of the foot in patients with critical limb ischemia: description of the technique. *Cardiovascular and interventional radiology*, 38(1):201–205, 2015.
- [23] K. D. Kurz, G. Ringstad, A. Odland, R. Advani, E. Farbu, and M. W. Kurz. Radiological imaging in acute ischaemic stroke. *European Journal of Neurology*, 23:8–17, 1 2016.
- [24] AA Konstas, GV Goldmakher, T-Y Lee, and MH Lev. Theoretic basis and technical implementations of ct perfusion in acute ischemic stroke, part 1: theoretic basis. *American Journal of Neuroradiology*, 30(4):662–668, 2009.
- [25] Heidi C Roberts, Timothy PL Roberts, Robert C Brasch, and William P Dillon. Quantitative measurement of microvascular permeability in human brain tumors achieved using dynamic contrast-enhanced mr imaging: correlation with histologic grade. *American Journal of Neuroradiology*, 21(5):891–899, 2000.
- [26] Leena M Hamberg, George J Hunter, Diane Kierstead, Eng H Lo, R Gilberto González, and Gerald L Wolf. Measurement of cerebral blood volume with subtraction three-dimensional functional ct. *American journal of neuroradiology*, 17(10):1861–1869, 1996.
- [27] Nizar A Mullani and K Lance Gould. First-pass measurements of regional blood flow with external detectors. *Journal of Nuclear Medicine*, 24(7):577–581, 1983.
- [28] Ernst Klotz and Matthias König. Perfusion measurements of the brain: using dynamic ct for the quantitative assessment of cerebral ischemia in acute stroke. *European journal of radiology*, 30(3):170–184, 1999.
- [29] Paul Meier and Kenneth L Zierler. On the theory of the indicator-dilution method for measurement of blood flow and volume. *Journal of applied physiology*, 6(12):731–744, 1954.
- [30] Leif Østergaard, Robert M Weisskoff, David A Chesler, Carsten Gyldensted, and Bruce R Rosen. High resolution measurement of cerebral blood flow using intravascular tracer bolus passages. part i: Mathematical approach and statistical analysis. *Magnetic resonance in medicine*, 36(5):715–725, 1996.
- [31] Longting Lin, Andrew Bivard, Timothy Kleinig, Neil J Spratt, Christopher R Levi, Qing Yang, and Mark W Parsons. Correction for delay and dispersion results in more accurate cerebral blood flow ischemic core measurement in acute stroke. *Stroke*, 49(4):924–930, 2018.

- [32] Kohsuke Kudo, Makoto Sasaki, Kei Yamada, Suketaka Momoshima, Hidetsuna Utsunomiya, Hiroki Shirato, and Kuniaki Ogasawara. Differences in ct perfusion maps generated by different commercial software: quantitative analysis by using identical source data of acute stroke patients. *Radiology*, 254(1):200–209, 2010.
- [33] Louise Strandberg, Pernilla Jonasson, and Maria Larsson. Evaluation of radiation doses using cone beam computed tomography in endovascular aortic repair and scoliosis procedures. *Radiation Protection Dosimetry*, 195(3-4):306–313, 2021.
- [34] Marije E. Kamphuis, Marcel J. W. Greuter, Riemer H. J. A. Slart, and Cornelis H. Slump. Quantitative imaging: systematic review of perfusion/flow phantoms. *European Radiology Experimental*, 4, 12 2020.
- [35] Ct perfusion phantom (gammex™ technology) - sun nuclear, <https://www.sunnuclear.com/products/ct-perfusion-phantom>.
- [36] Model 432 - ct perfusion phantom - gammex - peo, <https://gotopeo.com/nl/medical/radiotherapie/qa-fantomen-2/model-432-ct-perfusion-phantom-gammex/>.
- [37] Dce perfusion flow phantom, compatible with ct, mri pet, <http://www.simutec.com/products/dceperfusion.html>.
- [38] B Driscoll, H Keller, and C Coolens. Development of a dynamic flow imaging phantom for dynamic contrast-enhanced ct. *Medical physics*, 38(8):4866–4880, 2011.
- [39] Paul S Tofts, Gunnar Brix, David L Buckley, Jeffrey L Evelhoch, Elizabeth Henderson, Michael V Knopp, Henrik BW Larsson, Ting-Yim Lee, Nina A Mayr, Geoffrey JM Parker, et al. Estimating kinetic parameters from dynamic contrast-enhanced t1-weighted mri of a diffusable tracer: standardized quantities and symbols. *Journal of Magnetic Resonance Imaging: An Official Journal of the International Society for Magnetic Resonance in Medicine*, 10(3):223–232, 1999.
- [40] Hanneke van den Berg. Establishing requirements and a scoring algorithm for in-vitro brain perfusion flow models. *Bachelor Thesis University of Groningen*, 2021.
- [41] Hanneke van den Berg. Quantitative imaging: systematic review of brain perfusion/flow phantoms. *Bachelor Thesis Systematic Review University of Groningen*, 2021.
- [42] Axel Boese, Sebastian Gugel, Steffen Serowy, Jonas Purmann, Georg Rose, Oliver Beuing, Martin Skalej, Yiannis Kyriakou, and Yu Deuerling-Zheng. Performance evaluation of a c-arm ct perfusion phantom. *International journal of computer assisted radiology and surgery*, 8(5):799–807, 2013.
- [43] Christian Mathys, Konrad Rybacki, Hans-Jörg Wittsack, Rotem Shlomo Lanzman, Falk Roland Miese, Stephan Macht, Sven Eicker, Gerd Meyer zu Hörste, Gerald Antoch, and Bernd Turowski. A phantom approach to interscanner comparability of computed tomographic brain perfusion parameters. *Journal of computer assisted tomography*, 36(6):732–738, 2012.
- [44] Kazufumi Suzuki, Hiroyuki Hashimoto, Eiji Okaniwa, Hiroshi Iimura, Shingo Suzuki, Kayoko Abe, and Shuji Sakai. Quantitative accuracy of computed tomography perfusion under low-dose conditions, measured using a hollow-fiber phantom. *Japanese journal of radiology*, 35(7):373–380, 2017.
- [45] Patient measurements of the diameter of the a.tibialis posterior with angiographic images at the medisch spectrum twente performed by b. wermelink.
- [46] N Aggarwal, MM Paul, and M Mukherjee. Diameter of anterior cerebral artery-an anatomical study. 2013.
- [47] Achilles J Pappano and Withrow Gil Wier. *Cardiovascular physiology-e-book*. Elsevier Health Sciences, 2018.
- [48] J Aubrey, N Esfandiari, VE Baracos, FA Buteau, J Frenette, CT Putman, and VC Mazurak. Measurement of skeletal muscle radiation attenuation and basis of its biological variation. *Acta physiologica*, 210(3):489–497, 2014.
- [49] Francis H Glorieux. *Pediatric bone: biology & diseases*. Elsevier, 2003.
- [50] Ales Hrdlicka. Study of the normal tibia. *American Anthropologist*, 11(10):307–312, 1898.

- [51] Emile L Boulpaep. Arteries and veins. *Medical physiology*, 2:467–81, 2012.
- [52] Laleh Zarrinkoob, Khalid Ambarki, Anders Wåhlin, Richard Birgander, Anders Eklund, and Jan Malm. Blood flow distribution in cerebral arteries. *Journal of Cerebral Blood Flow & Metabolism*, 35(4):648–654, 2015.
- [53] Ferghal McVerry, Krishna Ashok Dani, Niall JJ MacDougall, Mary Joan MacLeod, Joanna Wardlaw, and Keith W Muir. Derivation and evaluation of thresholds for core and tissue at risk of infarction using ct perfusion. *Journal of neuroimaging*, 24(6):562–568, 2014.
- [54] KW Stock, SG Wetzel, PA Lyrer, and EW Radü. Quantification of blood flow in the middle cerebral artery with phase-contrast mr imaging. *European radiology*, 10(11):1795–1800, 2000.
- [55] Marc-André Weber, Wulf Hildebrandt, Leif Schröder, Ralf Kinscherf, Martin Krix, Peter Bachert, Stefan Delorme, Marco Essig, Hans-Ulrich Kauczor, and Holger Krakowski-Roosen. Concentric resistance training increases muscle strength without affecting microcirculation. *European journal of radiology*, 73(3):614–621, 2010.
- [56] Patient measurements of the perfusion of the lower extremities with angiographic images at the medisch spectrum twente performed by b. wermelink and l. van karnenbeek.
- [57] Håkan N Pärsson, Niklas Lundin, and Hans Lindgren. 2d perfusion-angiography during endovascular intervention for critical limb threatening ischemia—a feasibility study. *JRSM Cardiovascular Disease*, 9:2048004020915392, 2020.
- [58] F Simon, A Oberhuber, N Floros, P Düppers, H Schelzig, and M Duran. Pathophysiology of chronic limb ischemia. *Gefäßschirurgie*, 23(1):13–18, 2018.
- [59] Gene Y Cho, Sungheon Kim, Jens H Jensen, Pippa Storey, Daniel K Sodickson, and Eric E Sigmund. A versatile flow phantom for intravoxel incoherent motion mri. *Magnetic resonance in medicine*, 67(6):1710–1720, 2012.
- [60] Jyh-Wen Chai, Jeon-Hor Chen, Yi-Hsuan Kao, Jan-Ray Liao, Clayton Chi-Chang Chen, San-Kan Lee, and Woei Chyn Chu. Spoiled gradient-echo as an arterial spin tagging technique for quick evaluation of local perfusion. *Journal of Magnetic Resonance Imaging: An Official Journal of the International Society for Magnetic Resonance in Medicine*, 16(1):51–59, 2002.
- [61] Ju Hee Lee, Hyunhee Cheong, Seung Soo Lee, Chang Kyung Lee, Yu Sub Sung, Jae-Wan Huh, Jung-A Song, and Han Choe. Perfusion assessment using intravoxel incoherent motion-based analysis of diffusion-weighted magnetic resonance imaging: validation through phantom experiments. *Investigative Radiology*, 51(8):520–528, 2016.
- [62] Fdm vs. sla: Compare filament and resin 3d printers, <https://formlabs.com/blog/fdm-vs-sla-compare-types-of-3d-printers/>.
- [63] Guide to selective laser sintering (sls) 3d printing, <https://formlabs.com/blog/what-is-selective-laser-sintering/>.
- [64] Ellen G Hoeffner, Ian Case, Rajan Jain, Sachin K Gujar, Gaurang V Shah, John P Deveikis, Ruth C Carlos, B Gregory Thompson, Mark R Harrigan, and Suresh K Mukherji. Cerebral perfusion ct: technique and clinical applications. *Radiology*, 231(3):632–644, 2004.
- [65] Jörg Bredno, Mark E Olszewski, and Max Wintermark. Simulation model for contrast agent dynamics in brain perfusion scans. *Magnetic Resonance in Medicine*, 64(1):280–290, 2010.
- [66] Fernando Calamante, David G Gadian, and Alan Connelly. Delay and dispersion effects in dynamic susceptibility contrast mri: simulations using singular value decomposition. *Magnetic Resonance in Medicine: An Official Journal of the International Society for Magnetic Resonance in Medicine*, 44(3):466–473, 2000.

- [67] Hiroshi Ito, Iwao Kanno, Chietsugu Kato, Toshiaki Sasaki, Kenji Ishii, Yasuomi Ouchi, Akihiko Iida, Hidehiko Okazawa, Kohei Hayashida, Naohiro Tsuyuguchi, et al. Database of normal human cerebral blood flow, cerebral blood volume, cerebral oxygen extraction fraction and cerebral metabolic rate of oxygen measured by positron emission tomography with ^{15}O -labelled carbon dioxide or water, carbon monoxide and oxygen: a multicentre study in japan. *European journal of nuclear medicine and molecular imaging*, 31(5):635–643, 2004.

A | Appendix A: Phantom requirements

	Phantom set-up	Specifications	Imaging & Analyses
Anatomy/morphology	<ul style="list-style-type: none"> Macrovasculature Microvasculature target region - 10x10x5 cm Bone 	<ul style="list-style-type: none"> a. Tibialis posterior: 0.31 cm diameter. At least 3 branches A. Cerebralis anterior is 0.21 cm The target tissue region should have the same attenuation coefficient as muscle (-29HU to 150 HU) Diameter bone: 2cm, attenuation coefficient: 250 to 1000HU 	<ul style="list-style-type: none"> Volume analyses: ROI 1x1(x1) cm Compatible software (syngo.via)
Physiology	Blood flow <ul style="list-style-type: none"> Macrovasculature Microvasculature target region 	2D/3D situation <ul style="list-style-type: none"> Completely overlapping structures in one plane Partly overlapping structures in one plane No overlapping structures in one plane 	Produce time-intensity curves of macro- and microvasculature/ tissue perfusion similar to the ones in the lower extremities and brain <ul style="list-style-type: none"> Arterial input function Venous output function TTP, AUC, MTT Degree of perfusion based on clinical parameter
Patho-physiology	<ul style="list-style-type: none"> Collaterals Perfusion defect 	<ul style="list-style-type: none"> Both healthy and pathological situation present in the phantom 0:15:100% reduced flow 10% and 25% later contrast arrival 	
Overall	<ul style="list-style-type: none"> Standardized and reproducible set-up Applicable for both Siemens Artis Pheno C-arm, Siemens Artis Icono and CT perfusion 		

Fig. A.1 Phantom requirements. In this table anatomy/ morphology, physiology and pathophysiology are presented as separate categories on the one side, and requirements regarding the phantom set-up, specification, imaging, and analyses per category are presented on the other side. Overall requirements apply to all categories and are shown at the bottom of the table.

B | Appendix B: Comparison Chart

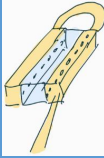
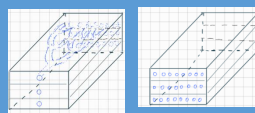
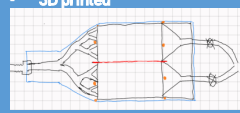
	Solution 1 - Macro circulation tube with small holes - Micro circulation sponge material - 3D printed 	Solution 2 - Macro circulation 3 x 3 Branches - Micro circulation 3 changeable modules sponge - Ecoflex material 	Solution 3 - Macro circulation 1 x 3 branches - Micro circulation 2 compartments sponge - Dividing wall - 3D printed 
Features			
Macro vasculature Incoming (0.31 cm) + outgoing artery	✓	✓	✓
Macrovasculature → microvasculature 3 branches		✓	✓
Macro vasculature → microvasculature Arrival time in the same range as in the lower extremities	✓	✓	?
Microvasculature HU muscle	✓	✓	✓
Microvasculature Time intensity curve parameters	?	?	?
Bone			
Flow macro circulation 30 mL/min – 120 mL/min	✓	✓	✓
Flow microcirculation 0.1-2.2 mL/min/100 gr	?	?	?
Collaterals simulation		✓	✓
Perfusion defect simulation	✓	✓	✓
2D/3D situation			
Healthy & Pathology in one view		✓	✓
Standardized and reproducible set-up	~✓	~✓	✓
Compatible with Siemens Artis Icono and Siemens Artis Pheno C-arm	✓	✓	✓

Fig. B.1 Comparison chart

C | Appendix C: Analyses method in Matlab

Function for ROI selection:

- Input: Squeezed Dicom file (width x height x # frames matrix uint16), info of Dicom file
- Output: ROIs, at the same position for all measurements
- 1. Read the squeezed Dicom file
- 2. Rotate the image to get the bottom line of the microcirculation compartment in a horizontal position
 - Select the left and right corner of the microcirculation compartment with getpts
 - Draw a line between these points
 - Determine the angle between the points
 - Rotate the image back with this angle
- 3. Calculate the size of one pixel with the real width of the phantom and the number of pixels between the left and right corners in the image of the phantom. Use the rule of Pythagoras.
- 4. Crop the microcirculation compartment of the image
 - Let MATLAB select a rectangle from the left corner that was earlier selected
 - The size of the rectangle in pixels is the real height and width of the microcirculation compartment divided by the ratio. The real height is 50 mm. The real width is 100 mm
 - Make a new image with only the microcirculation compartment by cropping this rectangle out of the original image
- 5. Select the ROIs out of the cropped image. First, determine the positions wanted in mm's and calculate them back to the pixel positions with the ratio

Function to rotate all the frames:

- Input: measurement, angle, DicomInfo
- Output: rotated image for all frames
- 1. Use the Dicom info to get the number of frames, the width of the image, and the height

- 2. Use trigonometry to calculate the new width and height of the rotated image
- 3. Rotate the images while looping over all the frames pre-allocate the new variable 'meting rotated' with a matrix of zeros with the size 'new width', 'new height', and the number of frames

Function to compute the average of the ROIs

- Input: the amount of frames, meting rotated, rectangles drawn with the ROI selection function
- Output: matrix with the average of the ROIs for each frame, table with the avg of ROIs, and column titles
- 1. Create a 1x(amount of ROIs) rectangle with all the rectangles that are drawn with the ROI selection function
- 2. Compute the average intensity for each ROI(j) in every frame (i)
 - Imcrop the rotated image with the position stored in the rectangle made with the ROI selection function
 - Compute the mean of the cropped image
 - Save this in the matrix with all ROIs and frames
- 3. Make a table of the matrix where the names of the ROIs are shown

Function to re-scale the average of the ROIs

- Input: the average of each frame for every ROI (computed in average ROI), DicomInfo
- Output: the scaled average of each frame for every ROI
- 1. Extend the matrix by adding the lowest and highest intensity of all the measurements together to each measurement
- 2. Use the re-scale function of MATLAB to re-scale the values between zero and one
- 3. Delete the last two rows of the matrix, to delete the added maximum and minimum values
- 4. Invert the values by subtracting them from one

Function to compute the time-intensity curves

- Input: DicomInfo and the scaled average of all the frames of one ROI (computed with the re-scaling function)
- Output: Time Intensity Curve
- 1. Compute the number of frames per second
- 2. Compute the time vector with the number of frames (this is a uint16 variable type, convert the variable to double) and amount of frames per second
- 3. Plot the time against the average intensity value of the ROI
- 4. Label the axes

- 5. Give the title, subtitle, and legend outside of the function

Function to compute the values of the time-intensity curves

- Input: The function of TIC values takes in the time and average intensity of the ROI per frame
- Output: The function computes the time of arrival (TOA), Time To Peak (TTP), Mean Transit Time (MTT), Slope of the curve (SOC) and the maximum intensity (MAX)
- 1. Compute the time vector with the number of frames (this is a uint16 variable type, convert the variable to double) and amount of frames per second
- 2. Compute the TOA by finding the time of the first local minimum of the time-intensity curve
- 3. Compute the maximum value and index of the maximum value
- 4. Compute the TTP, by subtracting the time of arrival from the time of the maximum value
- 5. Compute the SOC by dividing the maximum value minus the value at the time of arrival by the time to peak

Other possible values to compute from the measurements are:

- Mean transit time: we could compute the mean transit time, however, none of the measurements are long enough to get fully back to the starting value of the intensity
- Time to get back to half intensity: instead of mean transit time, the time to get back to half of the intensity
- Area under the curve: not ideal because the measurements have different lengths and do not get back to the starting intensity
- Time to peak from the starting point instead of from the TOA, this is usually done in the clinic, in our case, it is not desirable as we use different imaging systems with different contrast protocols, and the contrast injection timing differs

D | Appendix D: Workflow Syngo.via

1. The CT measurements are loaded into the software
2. None of the options for motion correction are selected
3. The option for brain segmentation is deselected
4. The HU values are set between -500 and 1000
5. The reference vessel needs to be defined. The incoming artery is defined as the reference vessel. The AIF is computed based on this vessel. The system will evaluate the pixel values of the reference vessel and segment all pixels with the corresponding value to be the reference vessel as well
6. The windowing is chosen based on visual appearance and improvements of the CT images
7. The ROIs are chosen. The software will show the AIF and TICs and TIC values of the ROIs